

THE INFLUENCE OF COLD-DEFORMATION ON THE
PERMEABILITY OF GASES (H_2, D_2) IN METALS
(Ni, α -Fe)

By

G.Egziabher Kahsay



A Thesis

Submitted in Partial Fulfillment of the
Requirements for the Degree of Master of
Science in Physics in the Addis Ababa University

June, 1987

CONTENTS

	PAGE
LIST OF TABLES	111
LIST OF FIGURES	v
INTRODUCTION	1
CHAPTER	
1. THE PERMEATION, DIFFUSION AND SOLUTION OF GASES IN NON-DEFORMED METALS	6
1.1 Consideration of the Permeation Mechanism of Gases in Solid Materials	6
1.2 Comparison to Literature	9
1.3 Analysis of Theoretical and Experimental Data on the Diffusion of Interstitial Impurities in Non- deformed bcc metals	16
1.4 The Evaluation of the Frequency Factor (D_0) by the Zener Model	20
1.5 Diffusion of Interstitial Impurities in Non- Deformed fcc Metals	24
1.6 Calculation of Solution Parameters of Interstitial Impurities in Non-deformed bcc Metals	25
1.6.1 Solution of Nitrogen in α -Fe	26
1.6.2 Solution of Carbon in α -Fe	29

CHAPTER	PAGE
2. THE INFLUENCE OF COLD-DEFORMATION ON THE PERMEABILITY, DIFFUSIVITY AND SOLUBILITY OF GASES IN METALS	31
2.1 INTRODUCTION	31
2.2 Experimental Data on the Influence of Cold-Deformat- ion on Hydrogen and Deuterium Permeability, Diffusivity and Solubility in Metals (Ni, α -Fe)	33
2.3 Critical Analysis of the Known Theoretical Interpretation of the Effect of Prior Cold-Deformation on Hydrogen Permeability, Diffusivity and Solubility in Metals	43
3. THE DEVELOPMENT OF THE MODEL, ANALYSIS AND INTERPRETATION OF THE EXPERIMENTAL DATA	53
3.1 INTRODUCTION	53
3.2 Description of Impurity Permeation, Diffusion and Solution in Metals with Dislocations	53
3.3 Analysis of the Experimental data by Using the Developed Model	60
3.4 Interpretation of the experimental Results	64
SUMMARY AND CONCLUSION	69
REFERENCES	74

LIST OF TABLES

	PAGE
1. Absolute Values of Permeability, Diffusivity and Solubility Calculated from Arrhenius Type Temperature Dependence Relation (eqns. 1.3 - 1.5)	10
2. Characteristics of the Arrhenius Type Temperature Dependence of Hydrogen Permeability in Non-deformed Nickel	11
3. Characteristics of the Arrhenius Type Temperature Dependence of Hydrogen Diffusivity in Non-deformed Nickel	12
4. Characteristics of the Temperature Dependence of the Coefficient of Hydrogen Solubility in Non-deformed nickel	13
5. Characteristics of the Arrhenius Type Temperature Dependence of Hydrogen Permeability in Non-deformed α -Fe	14
6. Characteristics of the Arrhenius Type Temperature Dependence of Hydrogen Diffusivity in Non-deformed α -Fe	15
7. Characteristics of the Temperature Dependence of the Coefficient of Hydrogen Solubility in Non-deformed α -Fe	15
8. Theoretical and Experimental Values of the Diffusion Parameters - Q_D , D_0 and $\frac{\Delta S}{R}$	23
9. Effect of Cold Work, Temperature and Flux Ratio on Deuterium Diffusivity in Nickel Calculated from Rise to steady State Permeation Measurements	35
10. The experimental data on deuterium Permeability, Diffusivity and Solubility in Nickel	38

List of Tables Contd.

	PAGE
11. The Experimental Data on Hydrogen Permeability, Diffusivity, and Solubility in Nickel	40
12. The Experimental Data on Hydrogen Permeability, Diffusivity and Solubility in α -Fe-0.16%C	42
13. The Results of the Treatment of the Experimental Data of Deuterium in Nickel.	61
14. The Results of the Treatment of the Experimental Data of Hydrogen in Nickel	62
15. The Results of the Treatment of the Experimental Data of Hydrogen in α -Fe-0.16%C.	63

LIST OF FIGURES

	PAGE
1. Permeation Mechanism of Gas in Metal	7
2. Octahedral ((a) - $(\frac{1}{2}\frac{1}{2}0)$, (c) - $(\frac{1}{2}00)$) and Tetrahedral ((b) - $(\frac{1}{2}\frac{1}{4}0)$) sites of an Interstitial impurity (\odot) in Non-deformed bcc Metals	17
3. The energy Barrier of Hydrogen Diffusion in Nickel	25
4. Physical Traps of Two-Energy-Levels	50
5. One of the Possible Dependences of Local Impurity Concentration in the NDSR (C_L) on the Volume Concentration of the Impurity (C)	58

ACKNOWLEDGEMENT

I offer my sincer and deepest gratitude to my advisor and instructor J.S. Netechaev, Dr. Sc. for his consistent supervision, limitless effort and dedication in guiding the work. His deep knowledge and rich experience in the field facilitated my progress in the thesis work and aroused my interest in the field for my further research work.

I would like to express my deep indebtedness to Prof. A.D. LeClaire (Harwell, UK) for his cooperation for having sent me some of his reprints.

I am also very grateful to W/ro Azeb Belay for her help in preparing the technical part of the thesis so neatly. I record my thanks to Ato Kidane Belay (Asmara University) and Ato Solomon Mulugeta for their cooperation in providing me with some indispensable materials for this work.

Finally, I gratefully acknowledge the assistance given by the Physics Department during my thesis work.

ABSTRACT

The ferro approach of the elastic Zener model has been corrected and developed for the evaluation of the elastic contribution to the thermodynamic characteristics of diffusion and solution of some interstitial impurities (H,N,C) in bcc metals (α -Fe). The Oriani approach and the Sakamoto general equation have been critically analyzed and developed. A theoretical description of the gases permeability including both the diffusivity and solubility with trapping effect and transport-by-dislocations effect has been done. This theoretical description has been used with respect to the known experimental data on the influence of prior cold-deformation on the gases (H_2, D_2) permeability diffusivity and solubility in some metals (Ni, α -Fe-0.16Zr). A model has been developed and implemented for finding true diffusion coefficients of impurities in the near-dislocation segregation regions (NDSR) in which there are some suitable experimental data.

Some information on the characteristics of the NDSR has been obtained which shows that the NDSR are not "easy path" for impurities diffusion. A relevant model of the NDSR structure has been discussed.

INTRODUCTION

When a wall of solid material such as non-porous metal or alloy separates two regions containing gas at different pressures, high pressure (P_1) and low pressure (P_2), there will generally be a dissolving of gas into the material (metal or alloy) on the high pressure (P_1) side, transport of the gas species across the wall and passage out by desolution in the low pressure (P_2) region. This process is called "Permeation". With the pressures maintained constant there is a build up with time to a constant "steady state permeation rate" through the wall.

Gases permeation through solid materials (metals or alloys), of fundamental interest as an aspect of solid state diffusion, is of considerable importance in very wide variety of technological applications.

Under many commonly occurring conditions of temperature and pressure, permeation behaviour can be fully described in terms of diffusion coefficients and equilibrium gases solubilities. In other words, permeation can be defined in terms of both thermodynamics and kinetics processes which bring about the thermodynamic equilibrium of the solubilities of gases (impurities) in the solid materials. This aspect will be considered in this work.

The permeation of gases in solid materials (metals or alloys) may occur by means of lattice diffusion, grain boundary diffusion or in the case of specimens undergoing plastic deformation by dislocations transport [1].

The significance of gases permeation in solid materials (metals or alloys) can be analyzed by the following aspects:

1) Permeation is a process which is realized by both thermodynamics and kinetics processes in the atomic level. Thus, the studies of permeation of gases in solids provide a unique way of investigating crystal structures, crystal defects, crystal properties, etc. From such studies of gases permeation in metals or alloys, some information about the characteristics of the near-dislocation segregation regions (NDSR) could be extracted. This possibility will be investigated in this paper.

2) Permeation plays an important role in many processes used to determine the structure, property, utility and strength of the solid materials; such as some phase transformations notably crystallization and recrystallization, corrosion, some mechanisms in semi-conductors and technologically important processes of deformation and destruction of metallic materials at high temperature and pressure.

Permeation of gases can take place in metals or alloys, oxides, inter-metallic compounds, semi-conductors, etc; in a wide range of temperature, pressure and other external conditions such as deformation. The influence of such external conditions (deformation) on gases permeability, diffusivity and solubility will be considered in this work.

Some of the most important and useful materials for the technological development achieved in this century are steels and some alloys based on Ni, Mo, Nb, Cr, Si, Al, etc.. The addition of some concentrations which are thermodynamically active elements (impurities) to these solid materials (alloys) will bring about a great influence on their technological properties, strength and utility.

For instance, the effect of hydrogen gas on the mechanical properties of metals, the rate of hydrogen motion in the metals and the thermodynamics

of hydrogen interaction with the metals have been intensively studied over many years [2,3]. In the present work more detailed consideration has been done on the permeability, diffusivity and solubility of H_2 , N_2 , C and D_2 in the metals - α -Fe, Ni and α -Fe - 0.16% C (steel). These impurities interact with the lattice imperfections in the matrix and change the property, structure, strength and utility of the metals or alloys under consideration. Thus, from these view points, it is worth studying the permeability, diffusivity and solubility of gases in solid materials (metals or alloys) for both academic and technological purposes.

Since hydrogen trapping behaviours are closely related to the resistance or susceptibility to hydrogen embrittlement of metals and alloys, there has been a continuing interest in these topics by many investigators [4]. Moreover, nickel is found out to be a suitable material to study the trapping of hydrogen at lattice imperfections such as impurities, dislocations, grain boundaries, etc., and the effect of oxide barriers on absorption, desorption and permeation under well defined surface conditions. This is due to the fact that the influence of surface contamination is reasonably small [5]. The permeability, diffusivity and solubility of H_2 in non-deformed nickel has been measured by surface sensitive methods such as permeation, electrochemical method, etc. [tables 2 - 4].

There has been a considerable number of work devoted to the interstitial hardening of bcc metals and alloys due to the impurities (N,C) interaction with dislocations. The corrosion process is also a serious problem nowadays. Its process is limited by permeation, diffusion and solution; this is due to the fact that the transport of the impurity (O_2) to the reaction zone is accomplished by these processes - permeation, diffusion and solution.

To sum up, the Ferro approach of the zener model has been corrected, developed and used for the evaluation of the elastic contributions for the diffusion and solution characteristics of some interstitial impurities in non-deformed bcc metals (α -Fe). The influence of prior cold-deformation on the permeability, diffusivity and solubility of gases (H_2, D_2) in metals (Ni, α -Fe-0.16%ZC) and the characteristics of the NDSR on these systems (D_2 in Ni, H_2 in Ni and H_2 in α -Fe-0.16%ZC) have been considered and treated indetailly.

The major components of this work are:

- 1) Collection and analysis of experimental data on the gases (H_2, N_2) permeability, diffusivity and solubility in non-deformed metals (Ni, α -Fe) with respect to finding the accuracy of the characteristics of temperature dependence of permeability, diffusivity and solubility. These quantities will be used as a standard for comparison with the data for deformed specimens.
- 2) Correction and development of the Ferro approach of the elastic Zener model for the evaluation of elastic contributions to the thermodynamic characteristics of diffusion and solution of interstitial impurities (H, N, C) in non-deformed metals (α -Fe).
- 3) Collection of experimental data on gases (H_2, D_2) permeability, diffusivity and solubility in cold-worked metals (Ni, α -Fe-0.16%ZC) and critical analysis of their known interpretation.
- 4) Development of the model for the description of the experimental data on the influence of cold-deformation on permeability, diffusivity and solubility.

- 5) Evaluation of the characteristics of the near-dislocation segregation regions for solution of H_2 and D_2 in Ni and H_2 in α -Fe-0.16%Zn (steel) by using the known experimental data on permeability, diffusivity and solubility in deformed and non-deformed specimens and the developed model.

CHAPTER I

THE PERMEATION, DIFFUSION AND SOLUTION OF GASES IN NON-DEFORMED METALS

1.1 The mechanism of permeation of gases in solid materials (non-porous metals or alloys) has been studied intensively by using various techniques (tables 2 and 7).

The permeation behaviour of gases in metals or alloys can be fully described in terms of the diffusion coefficients and equilibrium gas solubilities. Hence, permeation is defined by the product of solubility and diffusivity as:

$$\phi = \gamma D \quad (1.1)$$

where: ϕ , γ , D are the permeability, solubility and diffusivity coefficients respectively and $\gamma = \frac{C}{\sqrt{P}}$, C being the solubility at pressure P . Thus, permeability of gases in solid materials has a triple sense and can be expressed by both thermodynamic and kinetic processes.

The basic surface processes that are essential for permeation to occur are:

- i. the adsorption of molecules or atoms onto the surface from the gas phase and their desorption from the surface;
- ii. molecular dissociation on the surface to atoms and their recombination to molecules;
- iii. the absorption of the adsorbed atoms into solution in the surface layer of the solid and their reverse passage out of solution.

In some cases dissociation may occur simultaneously with adsorption so that processes (i) and (ii) become a single process; there is then no identifiable molecular phase on the surface. This is "direct dissociative chemisorption" and is believed to occur for instance, for hydrogen adsorption on many transition metal surfaces.

The net effect of gases permeation through solid materials (metals or alloys) is that gases at higher pressure (P_1) on the inlet side of the metals is transported through the metals or alloys to appear as atomic gases at a lower pressure (P_2) on the outlet side of the metals or alloys. In this case at a steady state the total amount flux (J) of gases per unit time which permeates through a plane sheet of specimen or surface area S and thickness b is expressed as (fig. 1).

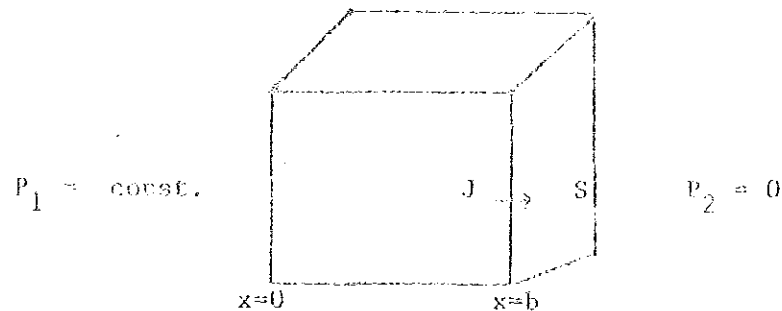


Fig. 1. Permeation mechanism of gas in metal

$$J = -DS \frac{dc}{dx} \quad (1.2a)$$

provided D is independent of concentration (C).

For a steady state case $\frac{dc}{dx}$ can be found by solving Fick's second law
 i.e $D \frac{d^2c}{dx^2} = 0$ (for steady state)

$$\therefore C(x) = Ax + B. \quad (1.2b)$$

Using the boundary conditions:

$$C_1(0) = \gamma\sqrt{P_1} = B \quad \text{and}$$

$$C_2(b) = \gamma\sqrt{P_2} = Ab + \gamma\sqrt{P_1} = 0, \quad \text{for } P_2 = 0,$$

the integration constants A and B can be determined. Hence, eqn. (1.2b)

becomes:

$$C(x) = -\frac{\gamma\sqrt{P_1}x + \gamma\sqrt{P_1}}{b}$$

and thus

$$\frac{dc(x)}{dx} = -\frac{\gamma\sqrt{P_1}}{b} \quad (1.2c)$$

substituting (1.2c) into (1.2a):

$$\phi = \mathcal{J} / \left(\frac{\sqrt{P_1}}{b} \right) \quad (1.2d)$$

where: $\phi = \gamma D$ and $\mathcal{J} = J/s$, \mathcal{J} being the flux density.

Therefore, the permeability of gases in metals can be equal to the flux density (\mathcal{J}) provided that the pressure gradient ($\sqrt{P_1}/b$) is equal to one.

The temperature dependence of gases permeability, solubility and diffusivity are expressed by the Arrhenius type relations of the form:

$$\phi = \phi_0 \exp(-Q_\phi/RT) \quad (1.3)$$

$$D = D_0 \exp(-Q_D/RT) \quad (1.4)$$

$$\gamma = \gamma_0 \exp(-Q_\gamma/RT) \quad (1.5)$$

$$\text{for } \phi_0 = \gamma_0 D_0 \quad (1.6)$$

and

$$Q_\phi = Q_D + Q_\gamma \quad (1.7)$$

where: $\phi_0, D_0, \gamma_0, Q_\phi, Q_D$ and Q_γ are the characteristics of the Arrhenius type temperature dependence of permeability, diffusivity and solubility respectively,

R is the gas constant and T is the temperature in Kelvin.

By using eqns. (1.3 - 1.5) and for given values of permeability, diffusivity and solubility characteristics, the absolute values of permeability, diffusivity and solubility of hydrogen and nitrogen gases in the non-deformed metals (Ni, α -Fe) at different temperatures can be evaluated (table 1).

1.2 COMPARISON TO LITERATURE

The literature of hydrogen permeability, diffusivity and solubility in non-deformed metals (Ni, α -Fe) is quite extensive. Tables (2-7) give a summary of the results of direct measurements that have been made for permeability, diffusivity and solubility characteristics in the non-deformed metals (Ni, α -Fe).

Because of the large number of variations on the different units possible, and since there is no universally preferred set of units, nearly every author has presented his results with a different set of units [5-8]. Thus, in order to compare the works of various authors, it has been necessary to derive a conversion factor in nearly every case to obtain the desired common units. This conversion process has been done in this work and the data of the different authors are listed in tables (2-7) after the conversion process is accomplished.

As can be seen from tables (2-7), the agreement of the results among the investigators is good.

TABLE 1: Absolute Values of Permeability, Diffusivity and Solubility Calculated From the Arrhenius Type Temperature Dependence Relation (eqns. 1.3-1.5)

System	T, K	ϕ	ϕ	D	γ	γ	References
		$\frac{\text{mol}(\text{H}_2, \text{N}_2)}{\text{ms}\sqrt{\text{MPa}}}$	$\frac{\text{at.fr. (H,N)}}{\text{s}\sqrt{\text{MPa}}}$	$\frac{\text{m}^2}{\text{S}}$	$\frac{\text{mol}(\text{H}_2, \text{N}_2)}{\text{m}^3\sqrt{\text{MPa}}}$	$\frac{\text{at.fr. (H,N)}}{\sqrt{\text{MPa}}}$	
H ₂	300	1.8×10^{-13}	1.2×10^{-18}	9.3×10^{-14}	1.9	1.3×10^{-5}	[7]
In	500	1.3×10^{-9}	8.7×10^{-15}	5.2×10^{-11}	24.6	1.6×10^{-4}	"
Ni	700	5.9×10^{-8}	3.9×10^{-13}	7.9×10^{-10}	72.6	4.8×10^{-4}	"
H ₂	500	6.6×10^{-11}	4.6×10^{-16}	1.5×10^{-8}	4.4×10^{-3}	3.1×10^{-8}	[8]
In	500	1.5×10^{-8}	1.1×10^{-13}	4.4×10^{-8}	3.4×10^{-1}	2.4×10^{-6}	"
α -Fe	700	1.6×10^{-7}	1.1×10^{-12}	7.0×10^{-8}	2.2	1.6×10^{-5}	"
N ₂	300	1.5×10^{-26}	1.9×10^{-31}	2.6×10^{-20}	5.6×10^{-7}	7.4×10^{-12}	[71, 72, 80]
In	500	1.2×10^{-18}	1.6×10^{-23}	5.2×10^{-15}	2.3×10^{-4}	3.0×10^{-9}	"
α -Fe	700	2.9×10^{-15}	3.7×10^{-20}	9.6×10^{-13}	3.0×10^{-3}	3.9×10^{-8}	"

TABLE 2 Characteristics of the Arrhenius Type Temperature Dependence of Hydrogen Permeability in Non-deformed Nickel.

Temperature Range in °K	Pressure in MPa	ϕ_0 ($\times 10^9$) at.fr.(H) m ² <hr/> S $\sqrt{\text{MPa}}$	Q_0 kJ/mol	Technique	References
623 - 873	0.101	3.9	53.3	Permeation disk	[9]
724 - 1150	0.101	5.3	55.3	Permeation Tube	[10]
523 - 623	"	8.1	56.4	" disk	[11]
623 - 873	"	6.6	53.1	" "	"
923 - 1093	"	2.6	57.6	" tube	[12]
673 - 1123	0.03 and 0.101	4.3	55.2	" "	[13]
473 - 593	0.101	7.9	55.0	" disk	[14]
633 - 1123	"	9.2	50.2	" "	[15]
353 - 523	"	3.0	54.8	" "	[16]
423 - 896	"	2.4	52.4	" "	[17]
313 - 463	"	4.3	51.8	" tube	[18]
297 - 773	0.101-0.303	4.7	54.7	" disk	[6]
300 - 500	0.04 and 0.6	5.2	55.3	-	[7]
393 - 703	-	2.3	52.0	-	[5]
297 - 1333	-	4.1	54.5	-	[19]

TABLE 3: Characteristics of the Arrhenius Type Temperature
Dependence of Hydrogen Diffusivity in Non-deformed Nickel

Temperature Range °K	D_0 ($\times 10^4$) m^2/s	Q_D kJ/mol	Technique	References
653 - 1259	4.5	35.9	Evolution	[20]
673 - 973	7.6	41.13	"	[21]
435 - 769	10.7	42.3	"	[22]
576 - 967	4.2	35.1	"	[23]
1243 - 1593	5.5	37.1	"	[24]
623 - 923	6.7	39.4	"	[25]
473 - 693	5.2	40.4	Permeation disk	[14]
673 - 873	4.4	36.3	Evolution	[26]
300 - 343	0.15	29.9	Permeation & ele.chem.	[27]
362 - 573	8.1	41.0	Permeation disk	[16]
503 - 623	5.3	40.0	"	[11]
623 - 873	4.2	37.2	"	"
573 - 923	5.0	40.4	Evolution	[28]
479 - 879	5.4	37.5	Absorption	"
1353 - 1669	4.7	31.8	Evolution	[29]
673 - 1273	7.0	49.4	"	[30]
623 - 973	6.1	40.5	Permeation disk	[17]
273 - 333	3.5	42.3	--	[31]
297 - 773	4.0	39.2	Permeation disk	[6]
300 - 500	7.0	39.5	Time lag and evolution	[7]
393 - 703	5.2	40.0	Permeation	[5]
273 - 328	3.5	42.4	Desorption	[31]
289 - 348	3.8	39.7	-	[32]
473 - 923	5.4	41.0	--	[33]
473 - 923	5.9	38.1	--	[34]
576 - 967	4.2	35.2	--	[35]

TABLE 4. Characteristics of the Temperature Dependence of the Coefficient of Hydrogen Solubility in Non-deformed Nickel

Temperature Range °K	γ_0 ($\times 10^3$) at. f.c. (H) $\sqrt{\text{MPa}}$	Q_γ kJ/mol	Technique	References
1007 - 1494	7.2	15.7	Absorption	[36]
576 - 967	6.0	14.8	Evolution	[23]
658 - 893	4.3	12.1	"	[25]
479 - 879	4.7	12.7	Absorption and Evo.	[28]
553 - 1123	4.3	12.5	Absorption	[15]
700 - 1300	3.5	10.2	"	[37]
1273 - 1726	17.0	25.6	"	[38]
300 - 500	7.2	15.8	"	[7]
-	5.4	12.0	-	[5]

TABLE 5: Characteristics of the Arrhenius Type Temperature
Dependence of Hydrogen Permeability in Non-deformed
 α -Fe.

Temperature Range °K	Pressure in MPa($\times 10^4$)	ϕ_0 ($\times 10^{10}$) $\frac{\text{at. fr. (H)} \cdot \text{m}^2}{\text{s} \cdot \sqrt{\text{MPa}}}$	Q_D KJ/mol	References
773-1173	253-1013	6.8	37.9	[40]
623-973	307-1013	6.1	35.1	[41]
399-966	31-31 $\times 10^4$	4.1	33.9	[42]
473-913	267	5.5	35.7	[43]
623-1073	1013	17.9	42.9	[44]
633-833	1013	5.4	35.3	[45]
573-1023	-	3.2	35.3	[46]
373-873	100-30659	4.6	34.3	[47]
503-673	-	5.2	35.1	[39]
273-333	10-1013	8.7	35.5	[48]
-	-	3.7	33.9	[8]
343-623	28-1021	6.2	33.8	[49]
297-583	200-49999	19.8	39.3	[50]
283-346	10-1013	6.4	35.0	[51]
322-779	4-628	8.5	35.6	[52]
533-773	200-6999	3.2	31.6	[53]
473-1123	-	5.7	34.2	[54]
343-673	1.3 $\times 10^{-5}$ -400	7.0	36.4	[55]
288-353	1000	5.2	34.3	[56]

TABLE 6: Characteristics of the Arrhenius Type Temperature Dependence of Hydrogen Diffusivity in Non-deformed α -Fe.

Temperature Range °K	D_o ($\times 10^8$) m^2/s	Q_D KJ/mol	Technique	Reference
423-1173	8.8	12.7	Evolution	[57]
283-373	22.0	12.9	-	[58]
673-1173	22.0	12.1	-	[59]
873-1053	14.0	-	Vacuum degassing	[60]
399-966	-	4.5	-	[42]
283-348	6.0	5.6	-	[61]
503-673	7.8	7.9	-	[39]
	22.0	6.7	-	[8]

TABLE 7: Characteristics of the Temperature Dependence of the Coefficient of Hydrogen Solubility in Non-deformed α -Fe.

Temperature Range °K	γ_o ($\times 10^3$) at. (H. (a)) \sqrt{MPa}	Q_Y KJ/mol	References
309-373	0.59	41.4	[58]
	1.7	27.2	[8]
503-673	6.7	27.2	[39]

1.3 ANALYSIS OF THEORETICAL AND EXPERIMENTAL DATA ON THE
DIFFUSION OF INTERSTITIAL IMPURITIES IN
NON-DEFORMED BCC METALS

The diffusion behaviours of interstitial impurities (H,N,C..) in bcc metals remains the subject of considerable interest in the areas of metal physics and materials science with respect to fundamental, experimental and technological aspects [62,63].

The mechanism of diffusion has been studied intensively [64-68]. As is well known, the problem can be reduced to that of a small atom moving at random in successive interstitial positions.

Quantitative measurements of the rate at which a diffusion process occurs are usually expressed in terms of the diffusion coefficient, the activation energy and the entropy or frequency factor, which are known as the diffusion characteristics. Since diffusion occurs as a result of the random motion of particles which are always thermally activated in solids, the diffusion coefficient thus becomes a very strong function of temperature as given by eqn. (1.4).

In [63] it has been shown that most of the known experimental data on the basic diffusion parameters - activation energy (Q) and frequency (or entropy) factors of the diffusion coefficients (D_0) of the impurities H,N,C, and O in fcc, hcp and bcc metals are compatible with the elastic zener model [67,68] with respect to the description of the relationship between D_0 and Q .

Different attempts have been made to evaluate the diffusion characteristics - Q and D_0 of interstitial impurities of diffusion in non-deformed bcc metals (α -Fe). For instance, in [69] an attempt has been made to evaluate the diffusion parameters (Q and D_0) of the interstitial impurities (H,N,C, B,O,) in the non-deformed bcc metals (α -Fe, Ta,Va,Nb,Mo) on the basis of the

elastic Zener model [67,68]. In this paper, it seems expedient to give some verifications of the results in [69] with respect to their applicability to the evaluation of the diffusion and solution characteristics of the impurities (H,N,C...).

Within the model [69], the diffusion process of the interstitial impurity in bcc metals (α -Fe) is considered as the transport (or jump) of an impurity atom from octahedral position ($\frac{1}{2}\frac{1}{2}0$) which is the origin state to the nearest octahedral position ($\frac{1}{2}00$) which is assumed to be the activated state at the constancy in temperature and volume (or pressure) of the matrix (fig. 2). But both these positions - ($\frac{1}{2}\frac{1}{2}0$) and ($\frac{1}{2}00$) are crystallographic equivalent sites in the sense that they all have identical environments. For both positions only two of the six nearest matrix neighbours should be displaced in the same manner in order to obtain the cavity size corresponding to the impurity atoms. That is why the elastic distortion energies are the same for both types of the octahedral positions. In other words, the two types of octahedral positions cannot be divided into origin and activated states of the impurities diffusion as was done in [69].

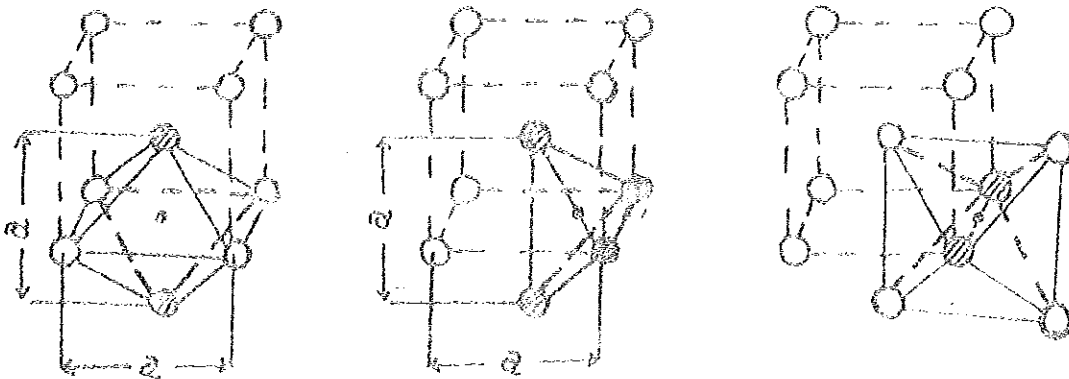


Fig. 2. Octahedral ((a) - ($\frac{1}{2}\frac{1}{2}0$), (c) - ($\frac{1}{2}00$)) and tetrahedral ((b) - ($\frac{1}{2}\frac{1}{4}0$)) sites of an interstitial impurity (*) in non-deformed bcc metals. The shaded circles (⊗) are the nearest matrix atom neighbours which should be displaced to obtain the cavity size of the impurity atom

For the heavy impurities (C,N,O,B) the tetrahedral position $(\frac{1}{2}\frac{1}{4}0)$ corresponds to higher elastic distortion energy in comparison with the octahedral positions in [59], since all the four nearest matrix neighbours should be displaced in order to form the impurity size cavity (fig. 1b). Thus, for the heavy impurities both types of octahedral positions can be considered as origin or final states of the impurity diffusion process, and the tetrahedral position $(\frac{1}{2}\frac{1}{4}0)$ as the activated state of the impurity diffusion process.

In the case of hydrogen impurity, the situation is entirely opposite. The tetrahedral cavity size is larger than the hydrogen impurity atom size, hence there is no elastic distortion energy for this site.

$$\begin{aligned} \text{i.e.} \quad r &= \left[\left(\frac{a}{4}\right)^2 + \left(\frac{a}{2}\right)^2 \right]^{\frac{1}{2}} - r_{\text{Fe}} \\ &= \left[\left(\frac{2.86}{4}\right)^2 + \left(\frac{2.86}{2}\right)^2 \right]^{\frac{1}{2}} \text{\AA} - 1.238 \text{\AA} \\ \therefore r &= 0.36 \text{\AA} \end{aligned}$$

where: r is the tetrahedral cavity size, a is the lattice parameter of α -Fe and r_{Fe} is the radius of α -Fe atom.

The value ($r = 0.36 \text{\AA}$) is larger than the radius of hydrogen ($r_{\text{H}} = 0.30 \text{\AA}$) atom impurity. Hence, the tetrahedral position can be considered as origin or final states of the impurity diffusion and the octahedral positions can be considered as the activated states of hydrogen impurity diffusion. Thus the elastic contributions to the activation free energy (ΔG) of hydrogen impurity diffusion can be connected with the external elastic work ($W < 0$) necessary to enlarge an octahedral cavity $(\frac{1}{2}\frac{1}{2}0)$ or $(\frac{1}{2}00)$ adjacent to an occupied tetrahedral cavity $(\frac{1}{2}\frac{1}{4}0)$ to the size of the interstitial impurity (H):

$$\Delta G = -(W)_{P,T} = \Delta E - T\Delta S \quad (1.8)$$

where: ΔE and ΔS are the elastic contributions to the activation energy and the activation entropy of the process respectively.

Within the elasticity theory, it has been shown [69] that

$$(W)_{V,T} \approx -1.3 N_{AV} \mu (d-h)^2 a \quad (1.9)$$

where: μ is the shear modulus of the non-deformed bcc metal (α -Fe) at T °K, N_{AV} is the Avogadro number, d is the diameter of the interstitial impurity atom, a is the lattice parameter of the non-deformed bcc metal (α -Fe) and h is the height of the octahedral cavity ($\frac{1}{2}\frac{1}{2}0$) or ($\frac{1}{2}00$) in the non-deformed bcc metal (α -Fe).

The evaluation of ΔE within the model [67,68] can be done as follows:

$$\Delta E = \left[\frac{\partial(\Delta G/T)}{\partial(1/T)} \right]_V = -(W)_{V,T} + T \left(\frac{\partial W}{\partial T} \right)_V \quad (1.20)$$

By using eqn. (1.9) it follows that:

$$\Delta E = 1.3 N_{AV} a (d-h)^2 \left(\mu - T \left(\frac{\partial \mu}{\partial T} \right) \right) \quad (1.21)$$

Thus the temperature dependence of μ can be represented as:

$$\mu = \mu_0 - T \left(\frac{\partial \mu}{\partial T} \right) \quad (1.22)$$

where: μ_0 is the shear modulus of the non-deformed bcc metal at 0 °K and $(\partial \mu / \partial T)$ is constant.

Hence we have;

$$Q = \Delta E = 1.3 N_{AV} a (d-h)^2 \mu_0 = -W_0 \quad (1.23)$$

where: Q is the elastic contribution to the activation diffusion energy and W_0 is the elastic work at 0 °K.

Eqn. (1.23) for the evaluation of Q is much more reasonable to the model [67,68] than the corresponding eqn. (9) in [69], which was obtained for the adiabatic process in the region containing about 10 atoms.

$$\begin{aligned} \text{i.e.} \quad dE &= \delta q - PdV - dW \\ &= Tds - PdV - dW \\ (dE)_{S,V} &= -dW \end{aligned}$$

$$\therefore (\Delta E)_{S,V} = -W = 1.3 N_{AV} a(d-h)^2 \mu_0 \left(1 - \frac{\beta T}{T_m}\right) \quad (1.24)$$

$$\text{for } T = \frac{\Delta E}{15R}$$

Particularly, it should be noted that in eqn. (9) in [69] the factor (which is about 15) before the gas constant was omitted without which the effective shear modulus at the local temperature ($T = Q/R$ [69]) will be negative which has no physical meaning.

1.4 THE EVALUATION OF THE FREQUENCY FACTOR (D_0)

BY THE ZENER MODEL

Within the model [67,68], the evaluation of the entropy factor (ΔS) can be done as follows:

$$\Delta S = -\left(\frac{\partial \Delta G}{\partial T}\right)_P = -\frac{Q}{T_m} \left[\frac{\partial(\Delta G/Q)}{\partial(T/T_m)}\right]_P \quad (1.25)$$

where T_m is the melting temperature of the metal and

$$Q = \Delta G_0 = (-W_0)$$

ΔG_0 being the change in free energy at 0 °K.

Taking into account eqns. (1.8 and 1.9) one can obtain [67,68]:

$$\Delta S = \beta Q/T_m \quad (1.26)$$

$$\text{where } \beta = -\left[\frac{\partial(\Delta G/Q)}{\partial(T/T_m)}\right]_V = -\frac{T_m}{T} \left(\frac{\partial Q}{\partial T}\right)_V \quad (1.27)$$

Therefore, the evaluation of the frequency factor (D_0) by using the known eqns. in [67-69] can be given as:

$$D_0 = \frac{1}{6} \psi a^2 \exp\left(\frac{\beta Q}{RT_m}\right) \quad (1.28)$$

where ψ is the order of the Debye frequency along the $\langle 100 \rangle$ direction in the non-deformed bcc metal, or

$$\psi = (Q/a^2 m)^{1/2} \quad (1.29)$$

m being the molar mass of the impurity.

The results of the evaluations of Q and D_0 by using eqns. (1.9 and 1.27-1.29) for hydrogen in α -Fe are given in table 8. The values of β , ψ_0 , h , a , d and ν have been used from [69].

The evaluated values of Q and D_0 for hydrogen diffusion in α -Fe (table 8) are of the same order as the experimental ones [42,61,70]. It shows that the elastic contributions to the characteristics Q and ΔS is considerable. Nevertheless, it is necessary to emphasize that much more complete consideration [62] of hydrogen diffusion in non-deformed bcc metals taking into account the electronic, lattice relaxation and zero point contributions give values of the activation energy (1-2) kJ/mol which is less than the experimental ones (4.8-9.3) kJ/mol [73] by about one order. The smallness of the calculated value (1-2) kJ/mol is mainly due to the underestimation of the short-range orthogonality repulsion experienced by hydrogen near the host-metal nuclei.

With respect to the heavy impurities C and N in non-deformed bcc metals (α -Fe), similar considerations can be made assuming the octahedral sites ($\frac{1}{2}\frac{1}{2}0$) or ($\frac{1}{2}00$) as origin or final states and the tetrahedral site ($\frac{1}{4}\frac{1}{4}0$) as the activated state, since the radius of these heavy impurities is larger than the tetrahedral cavity size of the diffusion process. The activation free

energy (ΔG) can be connected with the difference in the elastic distortion energy due to the interstitial atom in the activated position ($\frac{1}{2}\frac{1}{2}0$) and the origin position ($\frac{1}{2}\frac{1}{2}0$) or ($\frac{1}{2}00$).

By using the evaluation in [69], one can find that, within this model the elastic work at 0°K ($-W_0$) can be expressed as:

$$Q_{\text{exp}} \cong -W_0 \left(1 - \frac{\beta Q_{\text{exp}}}{15RT_m} \right) \quad (1.30)$$

where Q_{exp} is the experimental value of the activation energy.

Using 20% of the experimental value [69] for the activation energy (Q_{exp}) and $T_m = 1808$ °K for α -Fe, we get the values of C in α -Fe and N in α -Fe to be equal to 17 kJ/mol and 16 kJ/mol respectively. Hence, by using the values for C and N in α -Fe (evaluated using eqn. 1.30), the activation energies (Q) and frequency factors (D_0) can be evaluated (table 8).

The results of the evaluations of Q and D_0 for the systems C and N diffusion in α -Fe show that the elastic contributions are significant, but it is necessary to take into account the other contributions.

In principle, the total interaction free energy change can be assessed from a knowledge of the electronic and ionic rearrangements which occur in a solid when a solute atom migrates from some far-removed position in the lattice to position r . However, since the present state of the theory does not allow such a sophisticated analysis, the total free energy change is divided artificially into a number of pseudocontributions such as strain energy, electrostatic energy, electrochemical energy and vibrational entropy. For dilute solutions, the contributions are assumed to be mutually independent. Hence, the various components of ($\Delta G(r)$) are analysed individually and then algebraically summed to yield the total interactions of binding free energy.

TABLE 8: Theoretical and Experimental Values of the Diffusion Parameters - Q_D ,
 D_0 and $\Delta S/R$

System	Theoretical Values								
	Present Work			Work of [69] and [42]			Experimental Values		
	Q KJ/mol	$D_0 (X10^8)$ m^2/S	$\frac{\Delta S}{R}$	Q KJ/mol	$D_0 (X10^7)$ m^2/S	$\frac{\Delta S}{R}$	Q KJ/mol	$D_0 (X10^7)$ m^2/S	$\frac{\Delta S}{R}$
H_2 in α -Fe	5.3	13.0	0.15	5.4	0.92	0.15	5.6 [61] 11.5 [70] 4.5 [42]	0.6 [61] 1.1 [70] 0.4 [42]	-0.63 -0.38 -0.92
C in α -Fe	17.0	9.2	0.49	115.0	10.0	3.3	84.0 \pm 7.0 [71] 82.5 \pm 3.8 [70]	33.0 \pm 31.0 [70] 28.1 \pm 8.0 [70]	3.3 1.9
N_2 in α -Fe	16.0	8.2	0.46	96.0	10.0	2.7	76.0 \pm 3.0 [71] 76.5 \pm 0.5 [70]	4.5 \pm 3.3 [71,72] 30.0 $^{+52.0}_{-19.0}$ [70]	1.4 3.3

The electronic structure of the transition metals is so imperfectly understood and so little is known about the form of interstitial solutes in these metals that as yet no attempt has been made to calculate the activation energy and activation entropy from the fundamental principles. However, an empirical approach due to Zener and Wert [67] has proved very successfully in accounting for the experimental values of the activation entropy and the frequency factor (D_0). The activation free energy (ΔG) is the isothermal work done in moving an atom from an equilibrium position to the top of the adjacent potential barrier. A local dilatation of the lattice has been induced (by thermal fluctuation) to create a void in the solvent lattice sufficient to permit the passage of the interstitial solute atoms. The work done is largely associated with the elastic strain energy of this distortion, its magnitude depends upon the relative size of the solute and the matrix (solvent) atoms and the elastic constants of the matrix.

1.5 DIFFUSION OF INTERSTITIAL IMPURITIES IN NON-DEFORMED FCC METALS

Diffusion model for hydrogen in non-deformed fcc metals is totally different from the one described for non-deformed bcc metals. It is noted that in the high-temperature region the diffusion activation energy in the non-deformed fcc metals is typically (19.3-38.5)kJ/mol [73], which is much more than the calculated self-trapping energies in the octahedral sites. On the other hand, according to the calculations, self-trapping in the tetrahedral site is unprobable, and thus hydrogen would not be localized at the tetrahedral site during the activation process.

Neutron-diffraction data [75] for hydrogen diffusion in β -Ni shows unambiguously that the hydrogen atoms are localized in octahedral sites unlike to hydrogen atoms in bcc metals (α -Fe) which have tetrahedral sites.

The diffusion of hydrogen in non-deformed β -Ni has a potential energy barrier approximately equal to 35.5 kJ/mol (fig. 3). The width (2.5×10^{-10} m) is the distance between octahedral sites. The curvature of the potential well at the octahedral site is drawn to correspond to a frequency of

$$\nu = K\theta/h = 2.8 \times 10^{13} \text{ s}^{-1}$$

where: K is the Boltzman constant, θ is the Debye temperature in $^{\circ}\text{K}$ and h is Planck's constant.

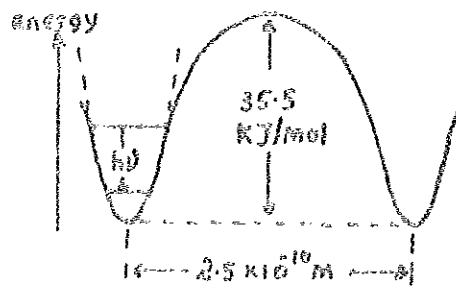


Fig. 3. The energy barrier of hydrogen diffusion in Nickel

It may be seen that for any likely shape of the potential energy barrier, the curvature at the top of the barrier will be less than in the well at the octahedral site. The implication of this observation is that tunneling effects are unimportant.

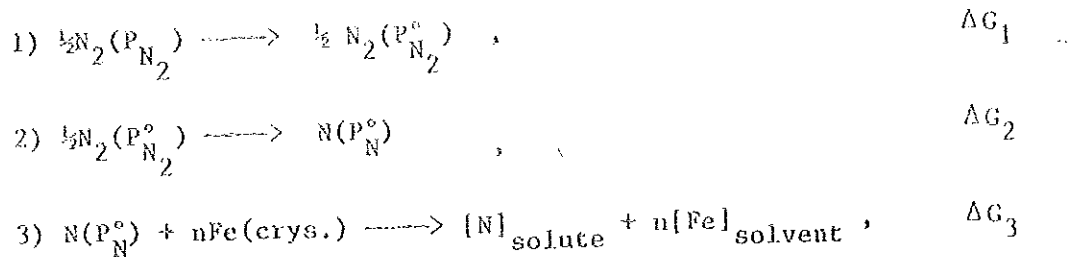
1.6 CALCULATION OF SOLUTION PARAMETERS OF INTERSTITIAL

IMPURITIES IN NON-DEFORMED BCC METALS.

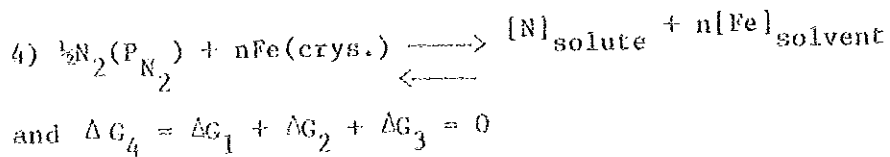
The Ferro approach [69] of the Zener model [67,68] can be used for the evaluation of the elastic contribution to the thermodynamic characteristics of the impurities (N_2, C) solutions in non-deformed bcc metals (α -Fe). Similar considerations have been done by some investigators [76,77]. Nevertheless, a detailed thermodynamic analysis is expedient.

1.6.1 Solution of Nitrogen in α -Fe

The solution process of N_2 in bcc metals (α -Fe) can be described as follows :



The net process of reactions (1-3) is:



where P_{N_2} is a given pressure of the molecular gas (N_2), $P_{N_2}^\circ$, P_N° are the standard pressures of the molecular and atomic gases respectively, ΔG_1 , ΔG_2 , ΔG_3 , ΔG_4 are the free energy changes of reactions (1-4) respectively.

The free energy change associated with the net process is Zero since reaction (4) is an equilibrium one. $n \gg 1$, since the gas solubility in the bcc metals (α -Fe) is small, i.e., dilute solutions are considered. Hence we can have:

$$\Delta G_1 = RT \ln(P_{N_2}^\circ / P_{N_2}) \quad (1.31)$$

$$\Delta G_2 = \frac{\Delta G_{\text{dis}}^\circ}{2} = \frac{\Delta H_{\text{dis}}^\circ(N)}{2} - \frac{T\Delta S_{\text{dis}}^\circ(N)}{2} \quad (1.32)$$

$$\Delta G_3 = RT \ln f_{[N]}^\circ (X_{(N)} / \eta) \quad (1.33)$$

$$f_{[N]}^\circ = \exp(\Delta H_{[N]} / RT) \exp\left(\frac{-\Delta S_{[N]}^{\text{xs}}}{R}\right) \quad (1.34)$$

where: $\Delta G_{\text{dis}}^{\circ}$, $\Delta H_{\text{dis}}^{\circ}$, $\Delta S_{\text{dis}}^{\circ}$ are the free energy, enthalpy and entropy changes of dissociation of N_2 respectively, $x_{(N)}^{\text{sol}}$ is the atomic fraction of the impurity (N) in the metal (α -Fe), $\nu(N) = 3$ is the number of octahedral sites per the matrix (solvent) atom, $f_{[N]}^{\circ}$ is the activity coefficient of the impurity atom in the dilute solution, $\Delta H_{[N]}$ and $\Delta S_{[N]}^{\text{xs}}$ are the relative partial molar enthalpy and excess entropy of the impurity in dilute solutions with respect to the atomic gas (N) at the standard pressure (P_N°).

As was done for instance by Oates [78], some standard state for the interstitial impurities could be chosen and different definition of the impurity activity can be used, where the finite number of the octahedral sites is taken into account. From the equilibrium condition of reaction (4), one can have:

$$f_{[N]}^{\text{eq}} = f_0 \exp\left(\frac{-\Delta H_{[N]}}{RT}\right) \sqrt{P} \quad (1.35)$$

$$\text{where: } \Delta H_{[N]} = \Delta \bar{H}_{[N]} + \frac{\Delta H_{\text{dis}}(N)}{2} \quad (1.36)$$

$$f_0 = \frac{v}{v P_N^{\circ}} \exp\left(\frac{\Delta S_{[N]}}{R}\right) \quad (1.37)$$

$$\Delta S_{[N]} = \Delta \bar{S}_{[N]}^{\text{xs}} + \frac{\Delta S_{\text{dis}}(N)}{2} \quad (1.38)$$

The quantities $\Delta \bar{H}_{[N]}$ and $\Delta \bar{S}_{[N]}$ are called the relative partial molar enthalpy and entropy of the impurity in the metal (α -Fe) solution with respect to the molecular gas (N_2) at the standard pressure ($P_{N_2}^{\circ}$) [79].

From the experimental data [80], on N_2 solubility in the metal (α -Fe), one can obtain the values of $\Delta \bar{H}_{[N]}$ and $\Delta \bar{S}_{[N]}$ as:

37.4 kJ/mol and 11.7 respectively.

By taking $\Delta H_{\text{dis}}(N_2) = 940$ kJ/mol [81] and $\Delta \bar{H}_{[N]} = 37.4$ kJ/mol, one can obtain

using equ. (1.36) the value of $\Delta \bar{H}_{[N]} = -433$ kJ/mol.

The elastic contribution to $\Delta \bar{H}_{[N]}^e$ in the metal (α -Fe) within the Ferro approximation [69] of the Zener model [67,68] can be evaluated by using eqns. (1.32) and (1.35) with respect to the solution process of ΔG_3 as:

$$\Delta \bar{H}_{(N)}^{el} = \left[\frac{d(\Delta G_3/dT)}{dT} \right]_P - W_0 \quad (1.39)$$

where W_0 is described by eqn. (1.23) and $\Delta \bar{H}_{(N)}^{el}$ is the elastic contribution to the relative partial enthalpy ($\Delta \bar{H}_{[N]}$),

by using the values of \bar{v}, μ_0, h, d and a for α -Fe and N from [69], one can find the value of $\Delta \bar{H}_{(N)}^{el} = 118$ kJ/mol. Thus, all the rest contributions ($\Delta \bar{H}^{re}$) can be evaluated by using the relation:

$$\Delta \bar{H}_{(N)}^{re} = \Delta \bar{H}_{[N]} - \Delta \bar{H}_{(N)}^{el} = 551 \text{ kJ/mol.}$$

The elastic contribution to $\bar{S}_{[N]}^{XS}$ for N in α -Fe within the Ferro approach [69] of the Zener model [67,68] can be evaluated using eqns. (1.18, 1.19, 1.25, 1.26 and 1.39) with respect to the solution process ΔG_3 . This excess entropy per impurity is called the intrinsic entropy of the impurity [77]. The elastic strain free energy per solute atom ΔG_3^* (exclusive of mixing entropy) can be expressed as:

$$\Delta G_3^* = \Delta \bar{H}_{[N]} - T \bar{S}_{[N]}^{XS} = -W_T^{el} \quad (1.40)$$

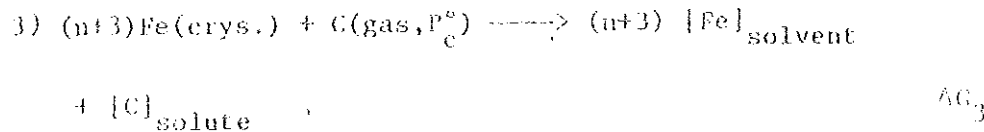
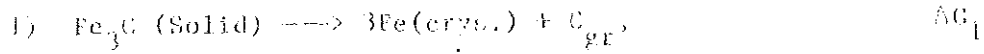
where W_T^{el} is given by eqn. (1.19). Hence, we have:

$$\frac{\bar{S}_{[N]}^{XS}}{R} = \frac{-c W_0}{RT_m} \quad (1.41)$$

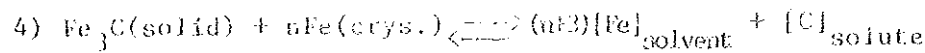
Thus, $\frac{\bar{S}_{[N]}^{XS}}{R} = 3.4$, and is the elastic contribution to the quantity,

1.6.2 Solution of Carbon in α -Fe

The solubility of carbon atoms in the metal (α -Fe) at a given temperature with respect to the carbide compound (Fe_3C) can be considered in the same manner as for N_2 in α -Fe:



The net process of reactions (1-3) is:



and

$$\Delta G_4 = \Delta G_1 + \Delta G_2 + \Delta G_3 = 0$$

i.e. the free energy change associated with the net process is zero since reaction (4) is an equilibrium reaction.

The free energy changes of the above reactions (1-3) can be expressed as:

$$\Delta G_1 = -\Delta G^\circ(\text{Fe}_3\text{C}) = -\Delta H^\circ(\text{Fe}_3\text{C}) + T\Delta S^\circ(\text{Fe}_3\text{C}) \quad (1.42)$$

$$\Delta G_2 = \Delta H^\circ(\text{sub.gr.}) - T\Delta S^\circ(\text{sub.gr.}) \quad (1.43)$$

$$\Delta G_3 = RT \ln f_{[\text{C}]}^\circ \left(\frac{X_{(\text{c})}}{n} \right) \quad (1.44)$$

$$f_{[\text{C}]}^\circ = \exp\left(-\frac{\Delta H_{[\text{C}]}^\circ}{RT}\right) \exp\left(-\frac{\Delta S_{[\text{C}]}^\circ}{R}\right) \quad (1.45)$$

where: $\Delta G^\circ(\text{Fe}_3\text{C})$, $\Delta H^\circ(\text{Fe}_3\text{C})$ and $\Delta S^\circ(\text{Fe}_3\text{C})$ are the standard quantities of formation of the carbide compound (Fe_3C), $\Delta H^\circ(\text{sub.gr.})$ and $\Delta S^\circ(\text{sub.gr.})$ are the

sublimation quantities of graphite, $X_{(c)}$ ($X_{(c)} \ll 1$) is the atomic fraction of the impurity (C) in the metal (α -Fe), $n(=3)$ is the octahedral sites per metal atom, $\Delta H_{[c]}$ and $\overline{\Delta S}_{[c]}^{xs}$ are the relative partial molar enthalpy and excess entropy of the impurity (c) in the dilute solution with respect to the atomic gas (c) at the standard pressure (P_c°).

From the equilibrium condition of reaction (4) we have:

$$X_{[c]}^{eq} = \gamma_0 \exp\left(\frac{-\Delta H_{[c]}}{RT}\right) \quad (1.46)$$

$$\text{where: } \Delta H_{[c]} = \overline{\Delta H}_{[c]} + \Delta H_{(sub.gr.)}^\circ - \Delta H_{(Fe_3C)}^\circ \quad (1.47)$$

$$\Delta S_{[c]} = \overline{\Delta S}_{[c]}^{xs} + \Delta S_{(sub.gr.)}^\circ - \Delta S_{(Fe_3C)}^\circ \quad (1.48)$$

$$\gamma_0 = \alpha \exp\left(\frac{\Delta S_{[c]}}{R}\right) \quad (1.49)$$

$\Delta H_{[c]}$ and $\Delta S_{[c]}$ are the relative partial molar enthalpy and entropy of the impurity (c) in the metal (α -Fe) solution with respect to graphite and carbide compound (Fe_3C).

From the experimental data [80] of carbide compound (Fe_3C) solubility in α -Fe, it follows

$$\Delta H_{[c]} = 40.6 \text{ kJ/mol and } \frac{\Delta S_{[c]}}{R} = -3.3.$$

By taking $\Delta H_{(Fe_3C)}^\circ = 22.6 \text{ kJ/mol}$ [80], $\Delta H_{(sub.gr.)}^\circ = 710 \text{ kJ/mol}$ and

$\Delta H_{[c]} = 40.6 \text{ kJ/mol}$; using eqn. (1.47) we have:

$$\overline{\Delta H}_{[c]} = -647 \text{ kJ/mol.}$$

Furthermore, the elastic contributions to $\Delta H_{[c]}^{el}$ and $\overline{\Delta S}_{[c]}^{xs}$ can be evaluated by using eqns. (1.39 and 1.41) and give values of 147 kJ/mol and 4.2 respectively.

Hence the rest contribution ($\Delta H_{[c]}^{re}$) = $\overline{\Delta H}_{[c]} - \Delta H_{[c]}^{el} = -794 \text{ kJ/mol}$.

The solubility of hydrogen in metals (α -Fe) can be analyzed by following the same procedure and has been considered in [78].

CHAPTER II

THE INFLUENCE OF COLD-DEFORMATION ON THE PERMEABILITY, DIFFUSIVITY AND SOLUBILITY OF GASES IN METALS

2.1 INTRODUCTION

In this chapter the influence of prior cold deformation on the gases permeability, diffusivity and solubility is discussed. The difference between prior cold-deformation and annealed (non-deformed) specimens is mainly connected with the dislocation density (ρ_d) and other defect concentrations.

The dislocation density (which is defined as the total length of dislocation (ρ_d) per unit volume (V) i.e. $\rho_d = \frac{\lambda_d}{V}$) in cold-worked specimens is of the order of $10^{15} - 10^{16} \text{ m}^{-2}$, i.e. by several orders higher than the dislocation density in the annealed specimen [82,83]. Such high dislocation density ($10^6 - 10^7 \text{ km/cm}^3$) corresponds to very large length of the dislocation networks (i.e. about $10^6 - 10^7 \text{ km}$ of the dislocation lines per cm^3 of the specimen).

By taking the diameter of the near-dislocation segregation region (NDSR) about $10 \times 10^{-10} \text{ m} - 100 \times 10^{-10} \text{ m}$ ($10 \text{ \AA} - 100 \text{ \AA}$) [82,83] and the dislocation density about $10^{15} - 10^{16} \text{ m}^{-2}$, one can obtain the maximum possible value of the volume (or atomic fraction) of the NDSR to be about 10^{-1} . This shows that the NDSR can considerably influence the impurity solubility of the gases in the metals and binding energy of the gases impurities in the NDSR; i.e. the local equilibrium concentration of the gases impurities in the NDSR can be higher by several orders than the equilibrium concentration of the impurities in the matrix. This is the so called the trap effect of the NDSR on the gas solubility [84,85].

The NDSR can influence the gas impurity diffusivity by the following two ways.

- 1) by pumping the diffusant impurity in the NDSR in accordance with the distribution law, it results in some diminishment in the gas diffusivity, this is the so called the trap effect of the NDSR on the impurity diffusivity (or the diffusion - with -trapping effect) [84,85].
2. The NDSR can influence the impurity diffusivity since the local diffusivity in the NDSR can differ so much from the impurity diffusivity in the metal (matrix); this is what is known as the transport - by - dislocations effect according to the nomenclature of Leblond and Dubois [85]. The later effect can result in both enhancement and diminishment in the net impurity diffusivity if the local impurity diffusivity in the NDSR is much higher or lower in comparison with the metal (matrix).

In most of the works [84-86], the transport-by-dislocations effect has not been taken into account without any satisfactory physical reasons. In this work it will be shown that in [87] this effect (i.e the transport-by-dislocations effect) was neglected inadequately.

One of the main objectives of the present work is to take into account the two above mentioned effects on both gases permeability and diffusivity in the cold-deformed specimens (Ni, α -Fe-0.16%Z). It will be shown that the treatment of the experimental data within the model, taking into account the two effects can give some information on both thermodynamic and kinetic, characteristics of the NDSR which are weakly studied till now [82]. This aspect is also one of the objectives of this work.

The known experimental data on the influence of cold-deformation on the permeability diffusivity and solubility for some systems, namely: D_2 in Ni, H_2 in Ni and α -Fe-0.16%C are considered in section 2.2.

2.2 EXPERIMENTAL DATA ON THE INFLUENCE OF COLD-DEFORMATION ON HYDROGEN AND DEUTERIUM PERMEABILITY, DIFFUSIVITY AND SOLUBILITY IN METALS (Ni, α -Fe)

In the work [7], the solubility, diffusivity and permeability of hydrogen, deuterium and tritium gases were measured in polycrystalline 99.98 and 99.995% Ni foils and rods at 300-500 °K. Various techniques for all three hydrogen isotopes at pressures between 0.04 and 0.4 MPa were used for the measurements, and both annealed (non-deformed) and cold-worked specimens were studied.

The specimens were vacuum-annealed at 1123 °K and furnace-cooled before testing. The foils were cold-rolled to 98% reduction in thickness than the annealed foils prepared from the same stock materials. Cold-work increases the dislocation density from approximately $10^{12} - 10^{16} \text{ m}^{-2}$, greatly increasing the potential trap density.

A summary and critical analysis of earlier permeation data [6] done by the authors [7] enabled them to conclude that the best equation for gases permeation (H_2 in Ni) is:

$$= 5.2 \times 10^{-9} \exp\left(\frac{-55300}{RT}\right) \frac{\text{at.fr(H)}\text{m}^2}{\text{s} \sqrt{\text{MPa}}} \quad (2.1)$$

The data for the permeability of non-deformed nickel to protium obtained in the work [7] from the current study agree closely with eqn. (2.1) as do the deuterium and tritium data when normalized by

multiplying by the square root of the mass number (M) [88]. Thus according to the experimental data [7] for the non-deformed specimen the gases permeability is described by:

$$\phi = \phi_0 \exp\left(\frac{-Q_\phi}{RT}\right) \frac{\text{at. fr. (H)} \text{ m}^2}{S \sqrt{MPa}} \quad (2.2)$$

$$\text{where: } \phi_0 = \frac{5.2 \times 10^{-9}}{\sqrt{M}} \text{ (at. fr. (H) m}^2\text{) / s} \sqrt{\text{MPa}}, \quad Q_\phi = 55.3 \text{ kJ/mol}$$

and M = 1, 2, 3 for hydrogen (protium), deuterium and tritium respectively.

According to the results in [7], cold work increases the permeability of hydrogen and its isotopes in a similar manner. This increase is attributed to dislocation networks effect providing short-circuit diffusion paths. No detailed analysis has been done about this effect by the authors [7]. In the work [7], two techniques have been used to calculate diffusivities: a time lag analysis [89] of permeation data and evolution of the time dependence of the rate of evolution from initially saturated specimens. Values calculated from the two sets of data were nearly identical for permeation or evolution rates near steady state. In [30] diffusivity values were selected by the authors [7] as the best estimate of true hydrogen diffusivity in non-deformed nickel. The tritium data obtained in [7] by offgassing techniques support this conclusion and indicate that the temperature dependence of hydrogen diffusivity in the annealed (non-deformed) specimen (nickel) can be described by:

$$D_L = \frac{7.0 \times 10^{-7}}{\sqrt{M}} \exp\left(\frac{-39500}{RT}\right) \frac{\text{m}^2}{\text{s}} \quad (2.3)$$

The effect of cold-work, temperature and flux ratio on deuterium diffusivity was calculated in the work [7] from rise to steady state permeation measurements. Some of the values for the flux ratio 0.8 are listed in table 9.

TABLE 9: Effect of Cold Work, Temperature and Flux Ratio
on Deuterium Diffusivity in Nickel Calculated
from Rise to Steady State Permeation Measurements [7]

T °K	$D_L (X10^{11})$ m ² /S	$D (X10^{11})$ m ² /S	$D_c (X10^{11})$ m ² /S	D/D_L	D_c/D_L
425	0.6913	0.6308	0.3716	0.9125	0.5375
494	3.278	2.991	2.618	0.9125	0.7376
500	3.697	2.361	2.588	0.9125	0.700
525	5.813	4.841	5.305	0.9125	0.9125

It was emphasized in [7] that the change in the apparent diffusivity (D_c) (ϵ being the degree of deformation) during rise to steady state permeation were significantly greater with foils cold-rolled to 98% reduction in thickness than for annealed foils prepared from the same stock material. As was mentioned before, cold-work increases the dislocation density from approximately $10^{12} - 10^{16} \text{ m}^{-2}$ greatly increasing the potential trap density and lowering the values of D_c/D for cold-worked foils with respect to annealed foils tested at the same temperature (table 9).

Trapping at dislocations has a negative binding energy, and thus the amount of hydrogen trapped at dislocations should decrease and D_c/D should increase with increasing temperature. The authors [7] have not made any quantitative description or evaluation of the characteristics of the NDSR. In this work this aspect will be analyzed.

The solubility coefficient (γ_0) and the heat of solution (Q_Y) for hydrogen solubility in non-deformed nickel were determined in [7] by using the relationships:

$$\Phi_0/D_0 = \gamma_0 \quad (2.4a)$$

$$\text{and } Q_Y = Q_\phi - Q_D \quad (2.4b)$$

hence for the annealed specimen (nickel), the following expression was obtained.

$$\gamma = 7.2 \times 10^3 \exp\left(\frac{-15800}{RT}\right) \frac{\text{at. fr. (H)}}{\sqrt{\text{MPa}}} \quad (2.4c)$$

The analysis of hydrogen transport in nickel [7] has shown that both trapping and short-circuit diffusion are present and have small but significant effects on permeation, evolution and absorption. Both effects appear to be associated primarily with the dislocation substructure of the specimen (nickel). It was noted that this behaviour was consistent with the predictions of the McNabb-Foster model of reversible trapping by dislocations [86]. In the terminology used in the work [85], these two effects are the diffusion-

with-trapping effect and the transport-by-dislocations effect. In the present work, the experimental data in table 10 on deuterium permeability, diffusivity and solubility in both cold-worked and annealed nickel will be quantitatively treated with respect to the two effects mentioned above in order to obtain the characteristics of the NDSR.

Similar experimental data on hydrogen permeability, diffusivity and solubility in both annealed and cold-worked nickel were obtained in the work [5].

The material used in this work [5] was a nominally 99.9% pure nickel sheet of thickness 110 μm . The specimen was cold rolled to a thickness of 90-100 μm , and cut into disk-shaped specimens $4 \times 10^{-2} \text{m}$ in diameter.

The permeabilities and diffusivities of hydrogen for both specimens (annealed and cold-worked) were measured by the permeation technique, in which hydrogen gas was applied under pressure to one side of the membrane and the hydrogen transport through the membrane was measured as a function of time.

In this work [5], a series of permeation measurements was carried out for the two specimens. A series of measurements was first made for the annealed specimen during stepwise cooling from 593 $^{\circ}\text{K}$ to 453 $^{\circ}\text{K}$, and further measurements were continued between 453 $^{\circ}\text{K}$ and 703 $^{\circ}\text{K}$. Similarly, a series of measurements was made for the cold-worked specimen during step wise heating from room temperature to 473 $^{\circ}\text{K}$. In each series of measurements, the system was first evacuated by holding the specimen at the measurement temperature until no further change in the background hydrogen partial pressure was observed. Hydrogen was then introduced into the reservoir, and the transport was measured as a function of time. The hydrogen pressure adopted was 0.01 MPa for the annealed specimen and 0.1 MPa for the cold-worked one.

TABLE 10: The Experimental Data [7] on Deuterium Permeability, Diffusivity and Solubility in Nickel

T, °K	$\epsilon = 0, \quad \bar{Q} \leq 10^{12} \text{ m}^{-2}$			$\epsilon = 0.98, \quad \bar{Q} = 10^{16} \text{ m}^{-2}$		
	$\gamma (\times 10^4)$ $\frac{\text{at. fr. (H)}}{\sqrt{\text{MPa}}}$	$D (\times 10^{11})$ m^2/s	$\phi (\times 10^{15})$ $\frac{\text{at. fr. (H) m}^2}{\text{s} \sqrt{\text{MPa}}}$	$\gamma_g (\times 10^4)$ $\frac{\text{at. fr. (H)}}{\sqrt{\text{MPa}}}$	$D_g (\times 10^{11})$ m^2/s	$\phi_g (\times 10^{15})$ $\frac{\text{at. fr. (H) m}^2}{\text{s} \sqrt{\text{MPa}}}$
425	1.5	0.63	0.94	4.2	0.37	1.6
494	2.6	3.0	7.9	5.7	2.4	13.8
500	2.8	3.4	9.4	6.4	2.5	16.3
525	3.4	5.4	18.0	5.8	5.2	30.1

The results for the hydrogen permeability in the annealed specimen obtained by the authors [5] agree well with the "best fit" values deduced by Robertson [6] from many data reported previously. The experimental data for the permeability in annealed nickel obtained in this work [5] agree closely with the expression:

$$\phi = 2.3 \times 10^{-9} \exp\left(\frac{-52039}{RT}\right) \frac{\text{at. fr. (H)} \text{m}^2}{\text{s} \sqrt{\text{MPa}}} \quad (2.5)$$

Furthermore, it is noted that the permeability for the cold-worked specimen is larger than that of the permeability in the annealed specimen (table 11). This increase in permeability is attributed to hydrogen trapping effect at lattice imperfections introduced by cold-deformation.

The hydrogen diffusivity was also measured in the same work [5] from the time-lag for the absorption run for the cold-worked and annealed (non-deformed) specimens. The diffusivity for the annealed specimen extracted from the time-lag experiment was expressed by:

$$D = 5.18 \times 10^{-7} \exp\left(\frac{-3992}{RT}\right) \text{ m}^2/\text{s} \quad (2.6)$$

in good agreement with the diffusivity values in [6] and [90].

The solubility of hydrogen in the annealed specimen (nickel) which is derived from the experimental data for permeability and diffusivity in the annealed specimen by using equs. (1.1), (2.4a) and (2.4b) is given by:

$$\gamma = 5.38 \times 10^{-3} \exp\left(\frac{-12046}{RT}\right) \frac{\text{at. fr. (H)}}{\sqrt{\text{MPa}}} \quad (2.7)$$

The hydrogen solubility in cold-worked nickel [5] was discussed by taking into account the hydrogen trapping effect.

In this work [5], no quantitative analysis has been done on the characteristics of the NDSR for the system (H_2 in Ni) under consideration. In the present work, this aspect will be assessed in the treatment of the data in table 11.

TABLE 11: The Experimental Data [5] on Hydrogen Permeability, Diffusivity and Solubility in Nickel

T, °K	$\epsilon = 0$, $\rho_L \leq 10^{12} \text{ m}^{-2}$			$\epsilon \approx 0.2$, $\rho_L \approx 10^{16} \text{ m}^{-2}$		
	$\gamma (X10^4)$	$D (X10^{11})$	$\phi (X10^{15})$	$\gamma_\epsilon (X10^4)$	$D_\epsilon (X10^{11})$	$\phi_\epsilon (X10^{15})$
	<u>at.fr.(H)</u>	<u>m²/S</u>	<u>at.fr.(H)m²</u>	<u>at.fr.(H)</u>	<u>m²/S</u>	<u>at.fr.(H) m²</u>
	<u>√MPa</u>		<u>S√MPa</u>	<u>√MPa</u>		<u>S√MPa</u>
354	1.29	0.065	0.05	4.63	0.017	0.07
392	1.80	0.256	0.31	5.40	0.144	0.38
430	2.19	0.77	1.08	4.25	0.562	1.29
468	2.57	2.01	3.86	4.63	1.420	4.81

The other system where there are necessary experimental data on permeability, diffusivity and solubility is the hydrogen- α -Fe 0.16%C system which is much more important in technology than the hydrogen-nickel and deuterium-nickel systems considered above.

Hill and Johnson [39] exposed small cylinders of α -Fe-0.16%C (steel) to 0.101 MPa H_2 gas at 503 °K to achieve uniform hydrogen contents in the specimens. Some specimens had been swaged at room temperature to 60% reduction in area. The evolution of the hydrogen from the metal with the origin hydrogen content C_0 into vacuum was followed at various temperatures and the apparent diffusivity (D_ϵ) was calculated as per an earlier analysis from the time in which the hydrogen content of the specimen decreased to 0.1 of the initial value after the log rate-time curves become linear. In [39] the hydrogen solubility (C_ϵ) in the deformed specimen (α -Fe-0.16%C) at 0.101 MPa of pressure was also measured as a function of charging temperature. Thus, the permeability in the deformed specimen (ϕ_ϵ) is evaluated by the product of the diffusivity in the deformed specimen (D_ϵ) and solubility coefficient in the deformed specimen (γ_ϵ) i.e. $\phi_\epsilon = \gamma_\epsilon D_\epsilon$ where $\gamma_\epsilon = C_\epsilon / \sqrt{P}$; provided that D_ϵ is closed to the steady state values for different temperatures.

The solubility of hydrogen in annealed specimen (α -Fe-0.16%C) can be described by the equation established by Gonzalez [45]:

$$\gamma = 6.6 \times 10^{-3} \exp\left(\frac{-27170}{RT}\right) \frac{\text{at. fr. (H)}}{\sqrt{\text{MPa}}} \quad (2.8)$$

The values of γ which have been obtained are listed in table 12.

The results of hydrogen diffusivity in annealed specimen (D) are calculated from Gonzalez's [45] evaluation of the steady state permeability and from eqn. (2.8) yielding the expression [84]:

TABLE 12: The Experimental Data [39, 45, 84] on Hydrogen Permeability, Diffusivity and Solubility in α -Fe-0.16% C.

T (°K)	$e = 0, \quad \underline{Q} \leq 10^{13} \text{ m}^{-2}$		$e = 0.60, \quad \underline{Q} = 10^{15} - 10^{16} \text{ m}^{-2}$			
	γ ($\times 10^5$)	D ($\times 10^8$) m^2/S	ϕ ($\times 10^{13}$)	γ_g ($\times 10^3$)	D_g ($\times 10^{10}$) m^2/S	ϕ_g ($\times 10^{13}$)
	$\frac{\text{at.fr. (H)}}{\sqrt{\text{MPa}}}$		$\frac{\text{at.fr. (H)} \cdot \text{m}^2}{\text{S} \sqrt{\text{MPa}}}$	$\frac{\text{at.fr. (H)}}{\sqrt{\text{MPa}}}$		$\frac{\text{at.fr. (H)} \cdot \text{m}^2}{\text{S} \sqrt{\text{MPa}}}$
523	1.3	1.2	1.6	1.8	1.8	3.2
573	2.2	1.5	3.2	1.4	3.6	5.2
623	3.5	1.7	5.9	1.2	8.6	10.0
673	5.2	1.9	9.8	1.0	17.0	17.0

$$D = 7.8 \times 10^{-8} \exp\left(\frac{-7942}{RT}\right) \frac{\text{m}^2}{\text{s}} \quad (2.9)$$

The steady state permeability values in the annealed specimen [45] have been obtained by the product of solubility and diffusivity values in the annealed specimen (table 12). Thus, by looking at table ~ 12, one can easily observe that; the permeability in the deformed specimen (α -Fe-0.16% C) is much larger than the permeability in the annealed specimen by about two times, the solubility in the deformed specimen is higher than the solubility in the annealed specimen by about two orders and the diffusivity in the deformed specimen is smaller than the diffusivity in the annealed one by about two orders in the given temperature.

As in the previous cases (H_2 in Ni and D_2 in Ni), this effect can be connected with the influence of the NDSR. According to the experimental data [91,92], the dislocation density in the deformed specimen can be taken as $10^{15} - 10^{16} \text{ m}^{-2}$ and in the annealed specimens $\leq 10^{13} \text{ m}^{-2}$ (table 12).

Similar results with respect to hydrogen permeability and diffusivity in deformed and annealed α -Fe were also obtained [8]. In the present work, we shall make analysis only on the experimental data after Gonzalez [45], Hill [39] and Oriani [84] which are much more detail.

2.3 CRITICAL ANALYSIS OF THE KNOWN THEORETICAL INTERPRETATION OF THE EFFECT OF PRIOR COLD-DEFORMATION ON HYDROGEN PERMEABILITY, DIFFUSIVITY AND SOLUBILITY IN METALS

The anomalous behavior of hydrogen both to its solubility and diffusivity in cold-worked metals and alloys (steels) is well known and has been the subject of repeated investigations [39, 93-96]. At the present time there seems to be fair agreement that these phenomena are due to attractive interactions between the dissolved hydrogen atoms and structural imperfections developed by deformation.

The study of the interactions between dissolved hydrogen atoms and lattice discontinuities such as vacancies, dislocations, grain boundaries, voids, particle-matrix interfaces or foreign interstitial and substitutional atoms in iron and other metals is of great importance from both technological and academic view points and in particular in regard to hydrogen embrittlement susceptibility. Therefore, the influence of hydrogen trapping on hydrogen diffusivity and solubility has been studied by a number of investigators [39, 84, 86, 93, 94, 96-101].

Darken and Smith [93] were the first to suggest that dissolved hydrogen is impeded in its diffusion by imperfections in the lattice of a cold-worked steel and applied the theory of subscale kinetics, as modified by the assumption of local equilibrium, to the problem. A similar point of view has since been adopted by other workers [39, 86, 95]. McNabb and Foster [86] developed a more general modelistic formulation for the phenomenon of diffusion with accompanying trapping at one kind of trap; but the derived non-linear partial differential equations did not have a general analytic solution. Oriani [84] has reformulated their work [86] in the context of the assumption of local equilibrium for a restricted domain of degree of trap coverage.

Oriani [84] has given more specific treatment based on the local equilibrium hypothesis, to show how the relevant parameters may be evaluated from experimental, and to apply the theory to existing experimental data. Most of the modern works are compared and reduced to the McNabb-Foster [86] and Oriani [84] results. Because of this, it is expedient to consider the Oriani's [84] derivation in detail and to give some critical remarks.

Oriani [84] considered a lattice consisting of two kinds of sites for occupancy by hydrogen. The vast majority of sites are the ordinary or normal sites characterized by the normal enthalpy of solution ΔH° , with respect to an atmosphere of gaseous hydrogen with which the lattice may be brought into

contact. The minor fraction of the sites, to be called the extraordinary or trapping sites provide an energetically favoured environment for occupancy by hydrogen, so that the energy of binding ΔH_b is a positive quantity, ΔH_b being the change of enthalpy to transfer hydrogen from an extraordinary site to a normal site.

For the description of the experimental data the simplest distribution law of hydrogen atoms between the extraordinary and normal sites was assumed:

$$K = \frac{\theta}{\theta_x} \quad (2.10a)$$

where: K is the equilibrium constant given by

$$K = \exp\left(-\frac{\Delta H_b}{RT}\right) \quad (2.10b)$$

θ_x and θ are the fractional occupancies of the extraordinary or trapping sites and the normal lattice sites respectively which are assumed to be much less than one (i.e. $\theta_x, \theta \ll 1$).

The hydrogen concentrations upon normal lattice sites (C) and upon the extraordinary sites (C_x) can be expressed as:

$$C = N\theta \quad (2.11a)$$

$$\text{and } C_x = N_x \theta_x \quad (2.11b)$$

where: N and N_x represent, respectively, the number of normal and extraordinary sites per unit volume of the specimen.

The author [84] considered only the case when the ratio of extraordinary to normal sites ($\frac{N_x}{N} \ll 1$) is small. Hence, he assumed that trap population does not appreciably reduce the cross-section for diffusion in the normal lattice, and he expressed Fick's first law for the flux J in terms of the occupied normal site only, as:

$$J = -D \frac{dC}{dx} \quad (2.12a)$$

$$\text{or } J = -D \frac{dC}{dC_E} \frac{dC_E}{dx} \quad (2.12b)$$

where $C_E = C + C_x$, D is hydrogen diffusivity in the normal lattice and

$$D_{\epsilon} = D \frac{dC}{dC_{\epsilon}} \quad (2.13)$$

D_{ϵ} being the apparent or phenomenological diffusivity in the deformed specimen.

By using eqns. (2.10a, 2.11a and 2.11b), the apparent solubility (C_{ϵ}) in the deformed specimen can be expressed as:

$$C_{\epsilon} = C(1 + K \eta_x) \quad (2.14)$$

and

$$\eta_x = N_x/N \quad (2.15)$$

η_x ($\eta_x \ll 1$) being the volume fraction of the extraordinary sites.

From eqns. (2.13) and (2.14) one can obtain:

$$D_{\epsilon} = \frac{D}{1 + \eta_x K} \quad (2.16)$$

Eqns. (2.14) and (2.16) correspond to eqns. (16) and (13) in [84] respectively.

The apparent solubility coefficient (γ_{ϵ}) in the deformed specimen can be represented as:

$$\gamma_{\epsilon} = \frac{C_{\epsilon}}{\sqrt{p}} = \gamma(1 + K \eta_x) \quad (2.17)$$

where γ is the solubility in the annealed specimen and p is pressure in MPa.

The apparent permeability (ϕ_{ϵ}) in the deformed specimen is thus expressed by using eqns. (2.16) and (2.17) as:

$$\begin{aligned} \phi_{\epsilon} &= \gamma_{\epsilon} D_{\epsilon} = \gamma D = \phi \\ \text{i.e. } \phi_{\epsilon} &= \phi \end{aligned} \quad (2.18)$$

ϕ being the permeability in the annealed specimen.

Thus, within the frame work of Oriani's model [84], the results of hydrogen permeability in the deformed and annealed specimens are equal (equ. 2.18). This result is in contradiction with the experimental data described in the previous sections i.e. $\phi_{\epsilon} > \phi$ (Tables 10-12).

This contradiction can be connected with the transport-by-dislocations effect which was omitted in the Oriani's model [84]. Such assumption was formulated, for instance in the work [7]. Within the model [84], only diffusion with trapping effect was taken into account. A similar model was also developed in [102-106] and others.

As was pointed out in the preceding paragraphs the reason for neglecting the transport-by-dislocations effect by Oriani [84] was connected with small volume fraction of the extraordinary (or trapping) sites (i.e. $n_x \ll 1$); and hence it was assumed that the impurity diffusion occurs preferably through the normal sites. As will be shown for the system considered, the impurity concentration is so small that at reasonable dislocation density in cold-worked specimens, reasonable values of binding energy and cross-sectional size of the NDSR, the majority of the impurity atoms can be localized in the NDSR. It should be emphasized that in the case of localization of the majority of the hydrogen atoms in the NDSR, the apparent diffusivity can depend strongly on the local diffusivity of the impurity atoms in the NDSR. In other words, in this case the transport-by-dislocations effect should be taken into account. Thus, it is clear that Oriani's [84] motivations of neglecting the transport-by-dislocations effect are inadequate.

The necessity of taking into account both the diffusion-with-trapping-effect and the transport-by-dislocations effect was pointed out by Leblon

and Dubois [85]. The authors [85] have developed a general mathematical description of hydrogen diffusion in steels in the framework in which the transport-by-dislocations effect was not included. General diffusion equations from Boltzman - type transport equations were obtained on the basis of statistical treatment of the random movements of hydrogen atoms. These equations included both the diffusion-with-trapping effect and the non-uniform solubility effect which is important for the case of concentrated solutions; the transport-by-dislocations effect could not be included within the model [85]. From this model [85], the well-known McNabb-Foster [86] and Oriani [84] models were recovered by suitable approximations.

In the work of Sakamoto [87], a generalized approach has been used in which the matrix is considered to contain a multitude of "lattice defects" such as the tensile stress fields associated with dislocations, coherent and semicoherent grain boundaries, precipitate particles crack-tips, high angle grain boundaries, in coherent particles - matrix interfaces, voids, etc. The systematology of Park [107] has been followed in order to deduce corresponding diffusion flux equations. In this work [87] an analysis of the apparent diffusivity of hydrogen in the so called mixed trap and multiple physical trap models was carried out based on the classical diffusion theory and on the assumption of a system of low occupation solubility of hydrogen in a normal lattice and trapping sites and by taking into account that the trapping sites have not only the characteristics trap density and depth, but also a trap 'width' and that the 'normal' lattice sites and individual traps have characteristics trapping and release rate. It should be emphasized that in this consideration [87] both the diffusion-with-trapping effect and the transport-by-dislocations effect were taken into account in the proper way.

Generalized expressions for the temperature dependence of the apparent diffusivity of hydrogen in mixed trap and multiple physical trap models were

obtained (eqns. 18 and 43) in [87]. However, the resulting equations contain too many unknown factors to enable a comparison to be made of the experimental data with each model. It is generally difficult to distinguish between the trapping characteristics of different traps, because of the complexity inherent in the problem and the large number of associated parameters.

Thus, the model has been recasted by the author [87] in terms of a "two-energy-level" problem in order to facilitate comparison with experimental data. In the work [87], traps were represented by an "averaged" and "effective" trap t as a suitable for individual traps. Hence, the associated parameters in this case are regarded as the effective quantity averaged over the region related to all the traps. The generalized apparent diffusivity of hydrogen in the trap model of "two-energy-level" both for the mixed trap model and the multiple physical trap model (fig.4) is given by:

$$\begin{aligned}
 D_E &= \frac{D_\ell^\circ \exp\left(-\frac{E_\ell}{RT}\right)}{\frac{\Delta G_{t,\ell}^\ddagger}{1-f_t} \left(1-f_t - f_t(1-f_{tx})\right)} \\
 &\times \left(1 - \frac{D_k^\circ}{D_\ell^\circ} \exp\left(-\frac{E_k - E_\ell}{RT}\right)\right) \\
 &+ f_t \exp\left(-\frac{\Delta G_{H,t,\ell}^\ddagger}{RT}\right) \left\{ (1-f_{tx}) \frac{D_p^\circ}{D_\ell^\circ} \exp\left(-\frac{E_p - E_\ell}{RT}\right) \right. \\
 &\left. + f_{tx} \frac{D_x^\circ}{D_\ell^\circ} \exp\left(-\frac{E_x - E_\ell}{RT}\right) \right\} \quad (2.19)
 \end{aligned}$$

where: D_ℓ° , D_k° , D_p° and D_x° are the frequency factors of the effective diffusivities, E_ℓ , E_k , E_p and E_x are the corresponding activation energies with regard to the jumping process of $\ell \longleftrightarrow \ell$, $\ell \longrightarrow t$, $\ell \longleftarrow t$ and $t \longleftrightarrow t$

intersites respectively (fig. 4); l being the lattice sites and t the trap sites; f_l is the volume fraction of normal lattice sites; f_t is the volume fraction of trapping sites, ($f_l + f_t = 1$); f_{tx} is the trap width i.e fraction of trapping sites from which impurity can jump with characteristics D_t and E_t in trap regions.

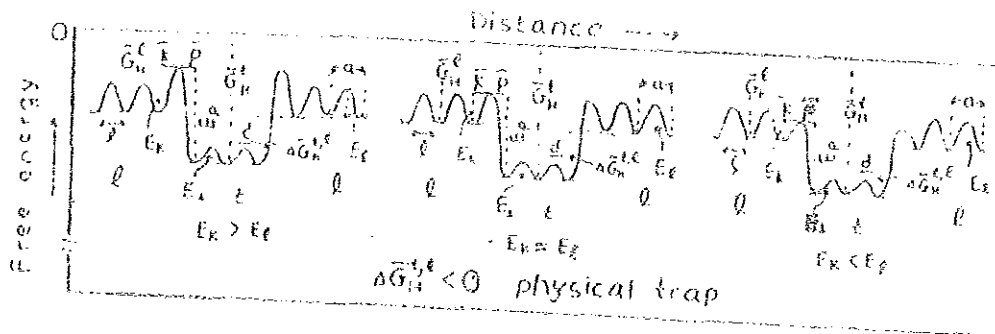


Fig. 4 Physical traps of two-energy-levels.

Sakamoto [87] made some inadequate reduction of eqn. (2.19) to the McNabb-Foster [86] and Oriani [84] models by taking the assumption, $f_{tx} = 0$, for the case if all the trapping sites are already saturated and donot influence the diffusion flux. If such assumption i.e $f_{tx} = 0$ were correct, then we could obtain from eqn. (2.19) the following expression:

$$D_E = \frac{D_l^0 \exp\left(-\frac{E_l}{RT}\right)}{1 + f_t \exp\left(-\frac{\Delta \bar{G}_H^{l,t}}{RT}\right)} \quad (2.20)$$

where the following assumptions are made, $f_t \ll 1$, $f_{tx} = 0$, $\frac{D_k^0}{D_l^0} = \frac{D_t^0}{D_l^0}$

and $(E_{\text{tr}} - E_{\text{tr}}) = (E_{\text{p}} - E_{\text{tr}} + \Delta G_{\text{H}}^{\text{tr}, \text{tr}})$ according to fig. 4.

Eqn. (2.20) is identical with eqn. (2.16) since: $D^{\text{tr}} \exp(-\frac{E_{\text{tr}}}{RT}) = D$,
 $f_{\text{tr}} = f_{\text{tr}}$ and $\exp(-\frac{\Delta G_{\text{H}}^{\text{tr}, \text{tr}}}{RT}) = K$ for $\Delta G_{\text{H}}^{\text{tr}, \text{tr}} = -\Delta H$.

The assumption $f_{\text{tr}} = 0$, for the case of the saturated trapping site should be expanded to the physically clear conclusion that in this case not only $f_{\text{tr}} = 0$ but also $f_{\text{tr}} = 0$. This means that in the case of the saturated traps, there is neither the diffusion-with-trapping effect nor the transport-by-dialocations effect. This aspect will be thoroughly discussed in this work. Here, it is relevant to add that physically, f_{tr} should be the same order or less than the quantity $(1-f_{\text{tr}})$, the sum of which corresponds to f_{tr} . Thus, if $f_{\text{tr}} = 0$ then $f_{\text{tr}} = 0$ as well. This immediately yields the following proper result for eqn. (2.19) in the case of saturated traps:

$$D_{\text{tr}} = D_{\text{tr}}^{\text{tr}} \exp(-\frac{E_{\text{tr}}}{RT}) \quad (2.21)$$

i.e. the apparent diffusivity (D_{tr}) is close to the true diffusivity (D) of the impurity of hydrogen atoms in normal lattice. The same result will be obtained in a different way in chapter - III.

In this section, it is expedient to give some proper reduction of eqn. (2.19) for the case of non-saturated trap regions with linear distribution law corresponding to low occupation probability of hydrogen in a normal lattice and trapping sites.

The following assumptions can be considered to reduce eqn. (2.19).

- 1) The volume fraction of the trap regions is negligible i.e. $0 \ll f_{\text{tr}} \ll 1$.
- 2) The boundary zones between the trap regions and normal lattice regions is of negligible thickness such that:

$$f_{tX} \approx 1 \quad \text{i.e.} \quad (1-f_{tX}) = 0$$

Hence, eqn. (2.19) can be reduced to:

$$D_C = \frac{D_\ell^\circ \exp(-E_\ell/RT)}{1+f_t \exp(-\frac{\Delta G_H^{t,\ell}}{RT})} \times [1+f_t \exp(-\frac{\Delta G_H^{t,\ell}}{RT})] \frac{D_\ell^\circ}{D_\ell^\circ} \exp(-\frac{E_\ell - E_\ell}{RT}) \quad (2.22)$$

Letting: $f_t = \eta_L$, $D_\ell^\circ = D_0$, $E_\ell = Q$

$$\exp(-\frac{\Delta G_H^{t,\ell}}{RT}) = K, \quad D_\ell^\circ = D_{0L} \quad \text{and} \quad E_\ell = Q_L$$

eqn. (2.22) can be expressed as:

$$D_C = \frac{D}{1+\eta_L K} \left[1 + \frac{\eta_L K D_0}{D} \right] \quad (2.23)$$

The same result as eqn. (2.23) will be obtained independently in Chapter - III.

In the conclusion of this chapter, it is expedient to emphasize once more that in the known theoretical considerations of the phenomenon the diffusion-by-dislocations effect is not taken into account without any satisfactory reasons as was done in the works [84-86, 102-107] or was omitted in the final expressions by doing inadequate reductions as in [87]. That why, it is indispensable to give some proper considerations analogous to Oriani's [84] approach but with a very important difference from [84] in the sense that it has taken into account not only the diffusion-with-trapping effect but also the transport-by-dislocations effect. This aspect is analyze in Chap. III.

CHAPTER III

THE DEVELOPMENT OF THE MODEL, ANALYSIS AND INTERPRETATION OF THE EXPERIMENTAL DATA

3.1 INTRODUCTION

Theoretical consideration of dislocation influence on gases diffusion, solution and permeation in cold-worked metals has been done in many of the works cited in chap. II; for instance [84-87, 108, 109]. In most of these works the so-called trap effect [85] of dislocation of impurity diffusion and solution has been discussed. At the same time the so-called transport-by-dislocations effect [85] is usually neglected in most of the works without any satisfactory explanations. In this chapter, special attention has been paid to the latter effect.

Based on the model which will be developed in this chapter, the analysis and interpretation of the known experimental data on gases (H_2, D_2) permeability diffusivity and solubility in both deformed and non-deformed metals (Ni, α -Fe) are discussed.

3.2 DESCRIPTION OF IMPURITY PERMEATION, DIFFUSION AND SOLUTION IN METALS WITH DISLOCATION

In order to extract the main features of the influence of dislocation on gases permeability, diffusivity and solubility the phenomenological consideration of the diffusion equation for an impurity in a crystal with dislocation decorated by impurity segregations seems expedient to consider.

Consider a one dimensional diffusion of an impurity along two neighbouring parallel regions of the same length having different cross-sectional areas (S_1, S_2), impurity concentrations (C_1, C_2) and diffusion coefficients (D_1, D_2). In the case of local equilibrium with respect to the impurity distribution between the two regions (which is adequate in the case of impenetrable partition) the total flux density can be described as:

$$J_{\Sigma} = -D_1 \eta_1 \frac{\partial C_1}{\partial x} - D_2 \eta_2 \frac{\partial C_2}{\partial x} \quad (3.1)$$

where: $\eta_1 = \frac{S_1}{S_1 + S_2}$ and $\eta_2 = \frac{S_2}{S_1 + S_2}$ are the volume fractions of the regions.

The total impurity concentration (C_{Σ}) can be represented as follows:

$$C_{\Sigma} = \eta_1 C_1 + \eta_2 C_2 \quad (3.2)$$

Thus, the total flux density (J_{Σ}) of the impurity is expressed as:

$$J_{\Sigma} = -D_{\Sigma} \frac{\partial C_{\Sigma}}{\partial x} \quad (3.3)$$

where D_{Σ} is the total apparent diffusivity of the impurity in the deformed specimen.

For the case $\eta_1 \approx 1$ and $\eta_2 \ll 1$, one can obtain from eqn. (3.2) the expressio

$$\frac{\partial C_1}{\partial x} = \frac{\partial C_{\Sigma}}{\partial x} \left(1 + \eta_2 \frac{\partial C_2}{\partial C_1}\right)^{-1} \quad (3.4)$$

By expressing eqn. (3.1) as:

$$J_{\Sigma} = -(D_1 + \eta_2 D_2 \frac{\partial C_2}{\partial C_1}) \frac{\partial C_1}{\partial x} \quad (3.5)$$

and by using eqns. (3.3 - 3.5), it follows that

$$D_{\Sigma} = \frac{D_1 + \eta_2 D_2 \left(\frac{\partial C_2}{\partial C_1}\right)}{1 + \eta_2 \left(\frac{\partial C_2}{\partial C_1}\right)} \quad (3.6)$$

In the approximation of the distribution law corresponding to a linear concentration dependence one can take:

$$\frac{\partial C_2}{\partial C_1} = K \quad (3.7)$$

where K can be called the effective distribution coefficient of the impurity.

The quantity $\frac{\partial C_2}{\partial C_1} = \text{Constant}$ can

differ considerably from the true equilibrium constant of the process (when one approximates a non-linear distribution law to a linear form within some concentration range). Hence the apparent diffusion coefficient of an impurity in a crystal (metal) with dislocations decorated with impurity segregation can be expressed as:

$$D_{\Sigma} = D_{\epsilon} = \frac{D}{1 + \eta_d K} + \frac{D_d \eta_d K}{1 + \eta_d K} \quad (3.8)$$

where D is the volume diffusion coefficient of impurity in a metal (crystal) containing no dislocation (non-deformed), D_d is the diffusion coefficient of an impurity in the NDSR, K can be the equilibrium constant of the impurity distribution process, η_d is the atomic (volume) fraction of the NDSR such that $\eta_d \ll 1$ and

$$\eta_d = \alpha b^2 \rho_d \quad (3.9)$$

ρ_d is the dislocation density in the crystal, b is the Burgers Vector and α is the number of atoms in a cross-section of the NDSR.

Eqn. (3.8) coincides with eqn. (2.23) which was obtained in this work by means of the proper reduction of eqn. (2.19).

The temperature dependence of D , D_d and K can be represented as:

$$D = D_0 \exp\left(-\frac{Q_D}{RT}\right) \quad (3.10)$$

$$D_d = D_{0d} \exp\left(-\frac{Q_d}{RT}\right) \quad (3.11)$$

$$K = \exp\left(-\frac{\Delta S_b}{R}\right) \exp\left(-\frac{\Delta H_b}{RT}\right) \quad (3.12)$$

where: D_{0d} is the frequency factor of the diffusion coefficient in the NDSR, Q_d is the activation energy of the NDSR; ΔS_b and ΔH_b can be the apparent binding entropy and enthalpy respectively.

Eqn. (3.8) is obtained under the following approximations.

- 1) There exists a local equilibrium between the NDSR and the volume solution.
- 2) The distribution law for the impurity corresponds to a linear concentration dependence (eqn. 3.7).

According to [109], the local equilibrium approximation can be used if $Dt \eta_d \geq 10^2$ holds, where t is the diffusion annealing time. For most of the experimental works quoted in this paper the inequality is valid.

The first term in the right hand side of eqn. (3.8) corresponds to the so-called diffusion-with-trapping effect and the second term to the transport-by-the dislocations effect according to the nomenclature of Leblond and Dubois [85].

First of all let us consider the limiting cases. When $\eta_d K \ll 1$, i.e. most of the diffusant atoms are located in the volume solution. Here, eqn. (3.8) corresponds to the Hart-Martlock equation [110] given by:

$$D_E = D + \eta_d K D_d \quad (3.13)$$

Eqn. (3.13) is used to describe the effect of segregation on the impurity diffusion enhancement due to the presence of dislocations [85]. In this limiting case the diffusion-with-trapping effect is negligible (i.e, the first term in eqn. (3.13) is close to D) and the transport-by-dislocations effect (i.e, the second term in eqn. (3.13)) can cause a considerable enhancement of the impurity diffusion if $D_L \gg D$, so that $\eta_L K D_L > 0$. This is a typical situation for the NDSR of the Cottrell cloud type [82].

In the other limiting case when $\eta_L k \gg 1$, i.e most of the diffusant is located in the NDSR, eqn. (3.8) can be written as:

$$D_\epsilon = \frac{D}{\alpha b^2 \eta_L K} + D_L \quad (3.14)$$

From this expression (eqn. 3.14), it follows that considerable diminishment of impurity diffusion (i.e $D_\epsilon < D$) can occur if $D_L \ll D$. Such a situation is not realized in the Cottrell cloud model where $D_L \gg D$ [82,107]. At the same time the desired result can occur for example when the structure of the NDSR is close to some compound structure possessing comparatively low impurity diffusivity. From eqn. (3.14) it follows that the transport-by-dislocations effect (in the case of $\eta_L K \gg 1$) can be neglected if $D_L \ll \frac{D}{\eta_L K}$, i.e. if the NDSR possess some structures with negligible impurity diffusivity. These aspects were not taken into account in many theoretical works [84 - 86].

In the work [87] the transport-by-dislocations effect was neglected by using the approximation of the saturated trap regions. In this case, however, the quantity $\frac{\partial C_2}{\partial C_1} = \text{Constant}$ in eqn. (3.8) has to be equal to zero, according to fig. 5. Then from eqn. (3.8), it follows that $D_\epsilon = D$; i.e there is neither the transport-by-dislocations effect nor the diffusion-with-trapping effect as it was discussed in Chap. II.

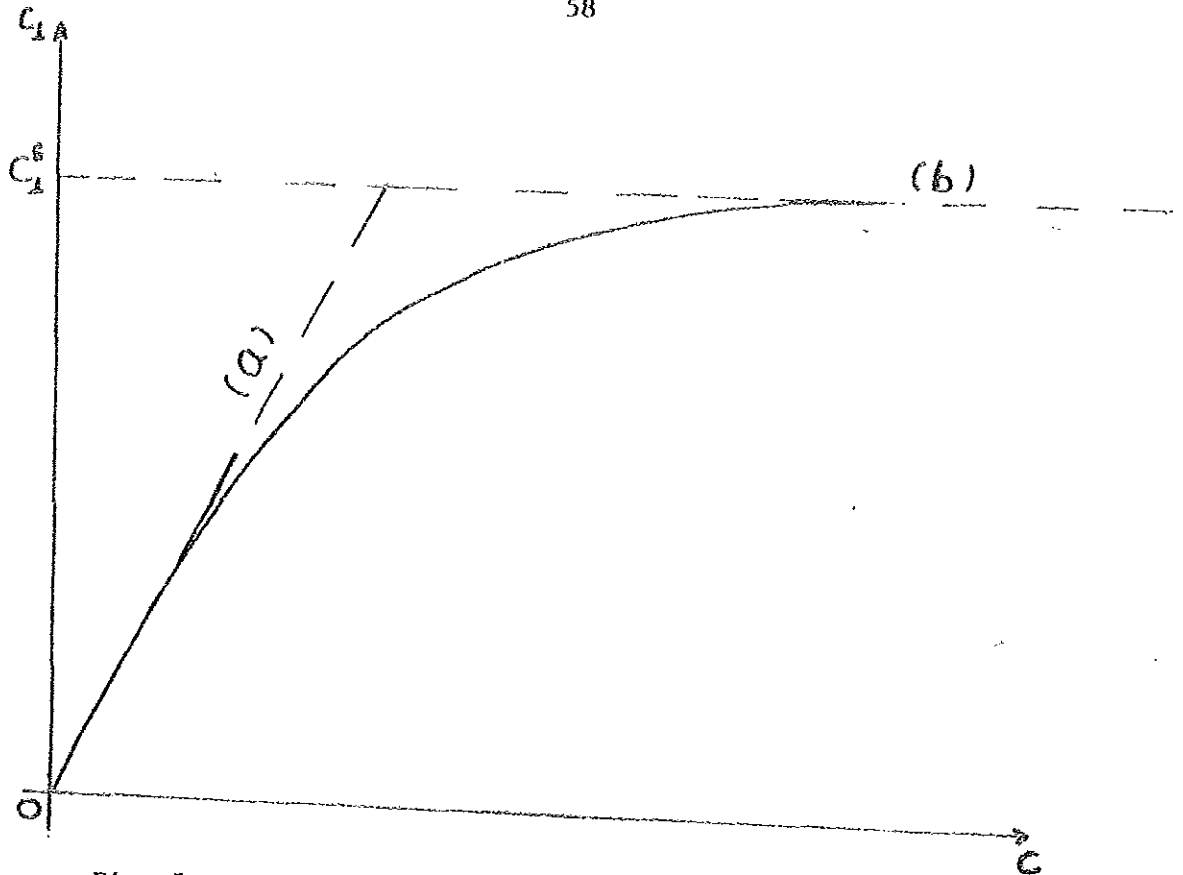


Fig. 5. One of the possible dependences of local impurity concentration in the NDSR (C_L) on the volume concentration of the impurity (C). Region (a) is the non-saturated case corresponding to the distribution law with the linear concentration dependence ($K = C_L/C$); region (b) is the saturated case corresponding to $\frac{\partial C_L}{\partial C} = 0$

The apparent solubility of an interstitial impurity in cold worked specimens can be described as:

$$C_E = C(1 - \eta_L) + C_L \eta_L \quad (3.15)$$

where C and C_L are the impurity solubility in the annealed specimen and the mean local concentration of the impurity in the NDSR respectively.

In the approximation of the impurity distribution law corresponding to the linear concentration dependence (eqn. 3.7), which is valid for dilute or ideal solutions, it could be assumed that:

$$C_L = KC \quad (3.16)$$

where K is described by eqn. (3.12).

Hence the solubility coefficient for a deformed specimen can be expressed as:

$$\gamma_\epsilon = \gamma(1 + \eta_L K) \quad (3.17)$$

where $\gamma_\epsilon = C_\epsilon/\sqrt{P}$ and $\gamma = C/\sqrt{P}$ from eqns. (3.8) and (3.17) we get:

$$\phi_\epsilon - \phi = D_L (\gamma_\epsilon - \gamma) \quad (3.18a)$$

$$\text{or } \phi_\epsilon/\phi = 1 + \eta_L K D_L/D \quad (3.18b)$$

where $\phi_\epsilon = \gamma_\epsilon D_\epsilon$, $\phi = \gamma D$.

$$\text{and } \gamma_\epsilon - \gamma = \frac{C_L \eta_L}{\sqrt{P}} \quad (3.19)$$

Eqn. (3.18a) shows that the difference in gases permeability in deformed and annealed specimens is connected with the local diffusion (D_L) and solubility (C_L) of impurity atoms in the NDSR and with the atomic fraction of the NDSR (η_L). Eqn. (3.18a) gives the unique opportunity of finding D_L from the experimental data on $\phi_\epsilon - \phi$ and $\gamma_\epsilon - \gamma$.

By using eqns. (3.8 - 3.18) for the treatment of the experimental data on the temperature dependence of ϕ_ϵ , ϕ , γ_ϵ and γ (or D_ϵ , D , C_ϵ , C) for specimens with known dislocation density (ρ_d) some parameters of the NDSR such as: the size factor (α), the local concentration (C_L), the thermodynamic and Kinetic characteristics of ΔH_b , D_{oL} and Q_L can be obtained. Hence, a suitable model of the NDSR structure can be developed. It can be emphasized that the NDSR structure is weakly studied till nowadays for the majority of the systems [82].

The illustration of such a treatment of literature (experimental) data for some systems (D_2 in Ni, H_2 in Ni and H_2 in α -Fe-0.16% C) is given in section 3.3.

3.3 ANALYSIS OF THE EXPERIMENTAL DATA BY USING THE DEVELOPED MODEL

In tables (10 ~ 12) the known experimental data on deuterium and hydrogen permeability, diffusivity and solubility in both cold-worked and annealed nickel [5,7] and hydrogen permeability, diffusivity and solubility in both cold-worked and annealed α -Fe-0.16% C [39,45,84] have been represented and discussed in Chapter II. This is rather a complete set of necessary experimental data for application of the model developed in section 3.2.

The results of the treatment of the experimental data of tables (10-12) are given in tables (13-15) respectively. The values of $\eta_L \exp(-\Delta S_b/R)$, ΔH_b and α (tables 13-15) have been obtained from the experimental data on γ and γ_c (tables 10-12), by using eqns. (3.15, 3.12 and 3.9). The values of C_L have been obtained from the expression given by; C_c/η_L or $\gamma_c\sqrt{P}/\eta_L$ (at $P = 0.101$ MPa), it follows from eqns. (3.16) and (3.17) in the approximation of $\Delta S_b \approx 0$. The same approximation has been used to evaluate α . It could be noted that the approximation ($\Delta S_b/R \approx 0$) is valid with the known accuracy for the solid state "reactions" (i.e. $\frac{\Delta S_b}{R} \approx 0, \pm 1$) [111]. It means that the evaluated values of the quantities (α and C_L) could be changed by several times.

The values of D (tables 13-15) have been obtained by using eqn. (3.18a) and the data from tables (10-12). The temperature dependence of D_L corresponds to the Arrhenius type equation described by eqn. (3.11), with the characteristics (D_{0L} and Q_L) given in tables (13-15).

TABLE 13: The Results of the Treatment of the Experimental Data of Deuterium
in Nickel [7] by Using eqns. (2.29-2.39)

$n_{\perp} e^{-\frac{\Delta S_b}{R}}$	ΔH_b KJ/mol	α (Q_{\perp}, m^{-2}) $d_{\perp} (X10^{10}, m)$	$C_{\perp} (X10^2)$ at 0.101MPa (T, °K)	$D_{\perp} (X10^{11})$ m^2/S (T, °K)	$D_{o_{\perp}} (X10^5)$ m^2/S Q_{\perp} KJ/mol	$D (X10^{11})$ m^2/S (T, °K)	$D_o (X10^7)$ Q KJ/mol
				0.21 (425)		0.63 (425)	
		10^2-10		1.9		3.0	
0.026	+0.008 -0.002	15.2 ± 5.7 $(10^{15}-10^{16})$	0.70 ± 2.20 $- 0.50$	(494)	1.6 ± 3.5 $- 1.5$	(494)	7.0
		25-8	(425-524)	2.3 (500)	55.9 ± 4.6	3.4 (500)	30.5
				4.4 (525)		5.4 (525)	

TABLE 14: The Results of the Treatment of the Experimental Data of Hydrogen in Nickel
[5] by Using eqns. (2.29-2.39)

$n_1 e^{-\frac{\Delta S_b}{R}}$	ΔH_b KJ/mol	a (Q , m^{-2}) d_1 ($\times 10^{10}$, m)	C_2 ($\times 10^2$) at 0.101MPa (T, °K)	D_1 ($\times 10^{11}$) m^2/S (T, °K)	D_{O_2} ($\times 10^5$) m^2/S Q_2 KJ/mol	D ($\times 10^{11}$) m^2/S (T, °K)	D_o ($\times 10^7$) m^2/S Q KJ/mol
				0.006 (354)		0.065 (354)	5.18
		10^2-10	$1.0+1.5$ -0.6				
0.015	15.4 ± 2.8	$(10^{15}-10^{16})$	(354-468)	0.02 (392)	0.28 $\frac{Q_2}{Q}$ -0.48	0.256 (392)	40.0
+0.019 -0.009		25-8		0.102 (430)	52.7 \pm 5.4	0.77 (430)	
				0.46 (468)		2.01 (468)	

TABLE 15: The Results of the Treatment of the experimental Data of Hydrogen in α -Fe-0.16%C
 [39,45,84] by Using eqns. (2.29-2.39)

$\frac{-\Delta S_b}{n_2 e \frac{R}{K}}$	ΔH_b KJ/mol	α ($\frac{g}{m^2}$) $d_1 (X10^{10}, m)$	$C_1 (X10^2)$ at 0.101MPa (T, °K)	$D_1 (X10^{11})$ m^2/s (T, °K)	$D_{O_1} (X10^6)$ m^2/s Q_1 KJ/mol	$D (X10^9)$ m^2/s (T, °K)	$D_0 (X10^8)$ m^2/s Q KJ/mol
				9.0 (523)		12.0 (523)	
	39.2±0.7	10^2-10	2.4±0.4				
0.017 +0.003 -0.002		$(10^{15}-10^{16})$		14.0 (573)	1.4 +3.5 -1.0	15.0 (573)	7.8 7.9
		25-8			42.8±1.9		
				35.0 (623)		17.0 (623)	
				78.0 (673)		19.9 (673)	

3.4 INTERPRETATION OF THE EXPERIMENTAL RESULTS

The treatment of the experimental data considered in section 3.3 gives the following three types of the characteristics of the NDSR in the systems under consideration.

Firstly; the quantity α is a geometrical parameter; i.e it gives the diameter of the crosssection of the NDSR.

For the three systems(D_2 in Ni, H_2 in Ni and H_2 in α -Fe-16%C), the obtained values of α are about 10^2 -10. Such a large error in the definition of the parameter α is connected with the fact that the dislocation density (ρ_d) in the specimens is known with accuracy of one or two orders of magnitude. Hence, the diameter of the NDSR can be evaluated by using the expression, $d_L = \sqrt{\alpha} b$. This yields the value of d_L to be about (8-25) Å for the three systems considered (tables 13-15).

The obtained values of d_L are rather reasonable since they correspond to the near core dislocation regions whose structural, thermodynamics and Kinetics characteristics can differ considerably from the characteristics of the matrix.

Secondly; the parameter C_L gives the local concentration (in at.fr.) of the impurity atoms in the NDSR. For the three systems considered, the obtained values of C_L is within the range of 0.029-0.002 at the pressure of 0.101 MPa and a given temperature range (tables 13-15). Such a large error in the definition of the local concentration (C_L) is connected with the parameter η_d from the temperature dependence of C_E/C . The errors of the definition of the η_d and C_L parameters can be minimized if the number of the experimental points for C_E/C as a function of temperature (T) is increased.

Nevertheless, the obtained values of C_L are by several orders of magnitude higher than the equilibrium concentration of the impurity atoms in the matrix at the given temperature and 0.101 MPa of pressure. For the system D_2 in Ni, the solubility of deuterium in the temperature range 354 °K - 525 °K and 0.101 MPa pressure lies within the range of 4.8×10^{-5} - 8×10^{-5} (table 10), for H_2 in Ni the solubility of hydrogen in the temperature range 354 °K - 468 °K and pressure 0.101 MPa lies in the interval 4×10^{-5} - 8×10^{-5} (table 11) and hydrogen solubility in α -Fe-0.16% C in the temperature range 354 °K - 673 °K and pressure of 0.101 MPa is 4.1×10^{-6} - 16.5×10^{-6} (table 12). It can be emphasized that both the matrix solutions ($C \sim 10^{-5}$ - 10^{-6}) and the NDSR solution of the impurities ($C_L \sim 10^{-2}$ - 10^{-3}) can be considered within the thermodynamic approximation of dilute solutions. This aspect will be used below.

Thirdly; the quantity ΔH_b is a thermodynamics parameter i.e it describes the binding enthalpy of the impurity atoms with the NDSR. For the systems D_2 in Ni and H_2 in Ni, ΔH_b is about (15.2 ± 5.7) kJ/mol (table 13) and (15.4 ± 2.8) kJ/mol (table 14) respectively. For H_2 in α -Fe-16% C ΔH_b is about (39.2 ± 0.7) kJ/mol (table 15).

These values of ΔH_b can be explained by taking into account one of the main contributions namely, $P_L \Delta \bar{V}$ where P_L is the local pressure in the NDSR and $\Delta \bar{V}$ can be taken as the partial molar volume of the impurity. At edge dislocations the local pressure (due to normal stress components) in the NDSR can be evaluated within the framework of the elasticity theory as follows:

$$P_L = \frac{1 + \nu^*}{1 - \nu^*} \left(\frac{2 \mu b}{3 \pi d_L} \right) \quad (3.21)$$

where: μ is the modulus constant $= 8.6 \times 10^{10} \text{ N/m}^2$ and ν^* is Poisson ratio $= 0.291$ for the matrix (α -Fe).

For the system H_2 in α -Fe-0.16%Zr, $d_{\text{L}} = 8 \times 10^{-10} \text{ m}$ and for the values of μ and ν^* given above, the local pressure (P_{L}) can be calculated by using eqn. (3.21) to be

$$P_{\text{L}} = 1.0 \times 10^{10} \text{ N/m}^2$$

According to [112], the partial molar volume of hydrogen in α -Fe is, $\Delta \bar{V} = 2.66 \times 10^{-6} \text{ m}^3/\text{mol}$. Thus,

$$P_{\text{L}} \Delta \bar{V} = 27.0 \text{ kJ/mol.}$$

This value is the same order as the experimental value of ΔH_{b} . The detailed consideration of this aspect is given in [113].

Similar treatment can be also done for the systems D_2 and H_2 in Ni.

Thus, on the basis of the results of the three parameters (α , C_{L} and ΔH_{b}), the possibility of a linear distribution law of the impurity atoms between the NDSR and the matrix within the approximation of the dilute solutions and $\Delta H_{\text{b}} = P_{\text{L}} \Delta \bar{V}$ can be explained. It should be noted that the assumption on a linear distribution law has been used in the derivation of the main equations (eqns. 3.8 and 3.16) of the model.

The characteristics of D_{L} , D_{OL} and Q_{L} can be considered as Kinetics, i.e. they can give some information on the local diffusivity characteristics of the impurity atoms in the NDSR. It is clear that these three diffusivity characteristics give some clue on the structure of the NDSR. In other words, by comparing the diffusion characteristics of the impurity atoms in the NDSR and the matrix, some information on the difference in their structure can be obtained. This information can be considered in connection with the previous parameters (α , C_{L} and ΔH_{b}).

The very new and important results obtained in the present work are that the local diffusivity (D_l) is less than the matrix diffusivity (D) by several times, the local activation energy (Q_l) is larger than the matrix activation energy (Q) i.e for H_2 in Ni 32%, D_2 in Ni 41% and H_2 in α -Fe-0.16%C 440% and the local diffusivity characteristics (D_{ol}) is larger than the matrix diffusivity characteristics (D_o) by 1-2 order (tables 13-15). This means that the NDSR in the systems under consideration cannot be considered as "easy path" of impurity diffusion as it is usually done by many investigators. For instance Louthan [7], Sakamoto [87], Yoshio [5] and others supposed that in the NDSR the impurity diffusion coefficient should be much higher than in the matrix and the impurity diffusion activation energy in the NDSR should be much less than in the matrix. Due to these assumptions the NDSR is usually considered as "easy path" for the impurity diffusion [7,82,87].

The very large value of Q_l for H_2 in α -Fe-0.16%C (steel) can be explained on the basis of [114]; that is, in this system, the NDSR structure can be close to the Fe_3C compound-like structure. This structure can possess much less values of hydrogen diffusivity with high activation energy.

For the systems D_2 in Ni and H_2 in Ni, the low values of the local impurity diffusivity and relatively high values of the local activation energy are explained by different crystal structure of nickel in the NDSR, i.e it can be face-centered-tetragonal (FCT) structure or hexagonal closed packed (HCP) structure instead of face-centered-cubic (FCC) structure in the matrix. This follows from the experimental data [115] in which the

presence of hydrogen atoms with concentration 10^{-2} - 10^{-3} leads to the stability of the HCP or FCT structures of Ni instead of FCC structure.

Thus, the analysis done in this work shows that all the experimental data on the influence of cold-deformation on H_2 and D_2 permeabilities, diffusivities and solubilities in Ni and α -Fe-0.16% C can be interpreted within the frame work of the model developed in the present work. The main result is connected with the possibility of the structure of the NDSR with low impurity diffusivity and high activation energy which is in contradiction with the widely used concept.

SUMMARY AND CONCLUSION

- 1) The known experimental data on hydrogen and nitrogen permeability, diffusivity and solubility in non-deformed metals (Ni, α -Fe) have been collected. It has been shown that the accuracy of Q_D , Q_D and Q_γ is $\leq 1\%$ and in the case of D_0 , D_0 and γ_0 it is $\leq 10\%$.

It has been shown also that, the known theoretical evaluation of D_0 , Q_D , γ_0 and Q_γ for hydrogen in metals (α -Fe) have low accuracy in comparison with the experimental values. For instance in one of the detailed and recent considerations [62], Q_D for H_2 in non-deformed metals is by one order less than the experimental ones.
- 2) The Ferro approach of the Zener model for the theoretical evaluation of Q_D and D_0 for interstitial impurities (H,N,C) in non-deformed bcc metals (α -Fe) is not proper with respect to the choice of the activated and origin states and the thermodynamic description of the diffusion process (Q_D). The satisfactory agreement of the evaluated values of Q_D and D_0 with the experimental values within the Ferro approach (Table 8) seems accidental. The proper application of the Zener model to the evaluation of Q_D and D_0 shows that the elastic contribution of Q_D for H_2 in α -Fe is close to the experimental value of Q_D and for N_2 and C in α -Fe it gives about 20% of Q_D experimental (table 8). The elastic contribution of the entropy factor (D_0) for the impurities (N,C) in α -Fe is about 10% of the experimental value of D_0 (table 8).
- 3) The Ferro approach of the Zener model has been used for a rough evaluation of the elastic contribution to the relative partial molar enthalpy (ΔH) and excess entropy ($\overline{\Delta S}^{XS}$) of the interstitial impurity (N,C) in dilute bcc metal solutions (α -Fe). It gives the values which differ from the experimental ones in sign and by several times in magnitude. The

experimental values of $\Delta \bar{H}$ and $\Delta \bar{S}^{XS}$ have been obtained on the basis of detailed thermodynamic analysis of the known experimental data.

- 4) The analysis of the known experimental data on the influence of prior cold-deformation on hydrogen and deuterium permeability, diffusivity and solubility in nickel and α -Fe-0.16%C crystals at temperature lower than the recrystallization ones show the existence of considerable effect lying out of the range of the experimental errors of the methods.

For instance; for D_2 in Ni at $T = 425$ °K: $\phi_{\epsilon}/\phi \approx 1.7$, $D_{\epsilon}/D \approx 0.6$ and $\gamma_{\epsilon}/\gamma = 2.9$ (Table 10). For H_2 in Ni at $T = 354$ °K: $\phi_{\epsilon}/\phi = 1.3$, $D_{\epsilon}/D = 0.3$ and $\gamma_{\epsilon}/\gamma = 3.8$ (table 11).

Similarly for H_2 in α -Fe-0.16%C at $T = 523$ °K $\phi_{\epsilon}/\phi = 2$, $D_{\epsilon}/D \approx 1.4 \times 10^{-2}$ and $\gamma_{\epsilon}/\gamma = 1.4 \times 10^2$ (table 12).

- 5) In the frame work of the known theories which are usually reduced to the Oriani model [84] with linear distribution law the diminishment of the impurity diffusivity ($D_{\epsilon}/D < 1$) and the increase of the impurity solubility ($\gamma_{\epsilon}/\gamma > 1$) in deformed specimens as compared to the annealed specimens are explained by the so-called trap-effect of the imperfections such as dislocations, cracks, etc. in the deformed specimens. According to Oriani's model with linear distribution law it follows that $\phi_{\epsilon}/\phi = 1$, i.e. the model [84] cannot explain the experimental result $\phi_{\epsilon}/\phi > 1$ (Tables 10-12). Some authors pointed out that for the explanation of the experimental data on $\phi_{\epsilon}/\phi > 1$, both the trap effect and the transport-

in one of the recent works [87], this effect (the transport-by-dislocations effect) has been inadequately neglected when the general expression was reduced to the applicable form.

- 6) The expression for D_{ϵ}/D for the impurity diffusivity which includes both the trap-effect and the transport-by-dislocations effect has been obtained (eqn. 3.8). This expression has been derived directly from the Fick's first law. It has been obtained also by the proper reduction of the general equation (eqn. 2.19).

For the description of the relation γ_{ϵ}/γ , the Oriani model [84] has been used. The combination of D_{ϵ}/D and γ_{ϵ}/γ allows to describe the increase in ϕ_{ϵ}/ϕ (eqn. 3.18b). Thus, the three main equations which can describe the experimental data on D_{ϵ}/D , γ_{ϵ}/γ and ϕ_{ϵ}/ϕ can be summarized as:

$$\begin{aligned} \text{i.} \quad D_{\epsilon}/D &= \frac{1 + \eta_L K \frac{D_L}{D}}{1 + \eta_L K} \\ \text{ii.} \quad \gamma_{\epsilon}/\gamma &= 1 + \eta_L K \\ \text{iii.} \quad \phi_{\epsilon}/\phi &= 1 + \eta_L K \frac{D_L}{D} \end{aligned}$$

- 7) From the temperature dependence of any pair of ϕ_{ϵ}/ϕ , D_{ϵ}/D and γ_{ϵ}/γ and by using the theoretical descriptions of the ratios of eqns. (i-iii) the characteristics of the near-dislocation trap regions which can be called as the near-dislocation-segregation regions (NDSR) have been obtained (Tables 13-15).

These characteristics of the NDSR are:

- a) The average diameter (d_L) of the NDSR
- b) The effective binding enthalpy (ΔH_b) of the impurity with the NDSR corresponding to the linear distribution law.

- c) The local concentration (C_L) of the impurity atoms in the NDSR.
- d) The local diffusivity (D_L) of the impurity atoms in the NDSR, the local activation energy (Q_L) and the frequency factor (D_{0L}) of the diffusion coefficient of the impurity atoms in the NDSR.

All these characteristics of the NDSR have been evaluated for the three systems (D_2 in Ni, H_2 in Ni and α -Fe-0.16%C) by using the experimental data for the systems under consideration (tables 13-15). The values obtained for the first three characteristics are consistent with the known theoretical descriptions of the near-core dislocation regions in metals. With respect to the fourth characteristics, the situation is rather different. It has been found out that the impurities diffusivities (D_L) in the NDSR are considerably less than the impurities diffusivities (D) in the matrix and the local activation energy (Q_L) in the NDSR is much greater than the activation energies (Q) in the matrix in the given temperature range (tables 13-15). Hence, it has been shown that the NDSR cannot be considered as "easy path" for the impurities diffusion unlike to the widely used aspect [17, 82, 87].

- 8) The characteristics of the NDSR in the systems considered show that the crystallographic structure of the NDSR can differ so much from the matrix. For H_2 in α -Fe-0.16%C (steel), it could be close to the carbide-like structure and the rest two systems could be close to the HCP or FCT structures than the FCC structure in the matrix.

Finally, it can be concluded that;

- 1) The Ferro approach of the Zener model has been corrected and used for the evaluation of the elastic contributions for both the diffusion and solution characteristics of some interstitial impurities (H,N,C) in non-deformed bcc metals (α -Fe).

- ii) For the first time a description of gases permeability including both the diffusivity and solubility with trapping effect and the transport-by-dislocations effect has been done. This theoretical description has been successfully used with respect to the known experimental data on the influence of the prior cold-deformation on the gases (D_2, H_2) permeability, diffusivity and solubility in some metals (Ni, α -Fe-0.16%C).
- iii) A new method has been developed and used for finding true diffusion coefficient of impurities in the NDSR by using eqns. (3.8-3.18). This method (model) has been applied in this work with respect to the three systems (D_2 in Ni, H_2 in Ni and α -Fe-0.16%C) for which there are suitable experimental data. Some new information on the NDSR for the systems has been obtained (tables 13-15) a relevant model has been discussed.

Thus, the present work contains some aspects which could be useful for the further studies of the peculiarities of the NDSR and development of the subject.

REFERENCES

1. J.K. Tien, A.W. Thompson, I.M. Bernstein, R.J. Richards Vol. 7A, No. 6 p. 821-9 (1976).
2. P. Cottrell, Prog. Mat. Sci. 9(1961)205.
3. D.P. Smith, Hydrogen in Metals, U. of Chicago Press, Chicago (1948).
4. M. Iino. Acta. Met. 1982, vol. 30, p. 367-75.
5. Yoshio Furuya, Ei-ji Hashimoto and Takao Kino: Jap. J. Appl. Phys. Vol. 23, No. 9, p. 1190-6(1984).
6. W. Robertson: Z-Metallk, Vol. 64, No. 6, p. 436-43. (1973).
7. M.R. Louthan, JR., J.A. Donovan and G.R. Caskey, JR. Acta. Met. Vol. 23, (1975)
8. N.R. Quick, Ph.D. Thesis Cornell. Univ. (1975).
9. A.A. Shcherbakova, J. Appl. Chem. USSR 29(1956) p. 955.
10. H.H. Girmes, Acta. Met. 7(1959)782.
11. Y.L. Belyakov and M.I. Ionov, Sov. Phys. Tech. Phys. 6(1961) 146.
12. E.A. Steigerwald, The Permeation of Hydrogen Through Constructional Materials. Report TRW-ER-4776 (NASA-CR-5119) Thompson-Ramo Wooldridge, Cleveland, Nov 30, 1961.
13. J.K. Gorman and W.R. Nardella, Vacuum 12(1962)19.
14. Y. EBISUZAKI, W.J. Kass and M.O' Keefe, J. Chem. Phys. 46(1967) 1378.
15. P.V. Gel'd, M.M. Shteinberg, Yu. P. Simakov and V.A. Gol'stov, Fiz-Khim, Mekhan. Mat. 2(1966)308.
16. J.A. Donovan, R.G. Derrick, A.H. Dexter and M.R. Louthan, Jr., Effect of Hydrogen Gas on Metals at -300 to 100°C Quarterly report. April-June 1971. Reprt DPST (NASA) -71-2, Dupont, Savannah River Lab. Aiken, S.C. Oct. 1971.
17. W. Fischer, Z. Naturforsch 22a(1967)1581.
18. R.H. Collins and J.C. Turnbull, Vacuum 11(1961)114.
19. A.D. LeClaire, diffusion and defect data, Vol. 36. p. 1-36 (1984).
20. M.L. Hill and E.W. Johnson, Acta. Met. 3(1955) 566.
21. C.E. Ransley and D.E. J. Talbot, Z. Metallkde 46(1955)328.
22. A.G. Edwards, Brit. J. Appl. Phys. 8(1957)406.
23. W. Eichenauer, Mem. Sci. Rev. Met. 57(1960)943.
24. L.M. Ryabchikov, Uer. Fiz. Zh. 9(1964) 303.
25. W. Eichenauer, W. Güsser and H. Witte, Z. Metallkde 56(1965) 287.

26. R. Dus and N. Smialowski, *Acta. Met.* 15(1967) 1611.
27. W. Beck, J. O'M. Bockris, M.A. Genshaw and P.K. Subramanyan, *Met. Trans.* 2(1971)883.
28. P. Combette and P. Azou, *Mem. Sci. Rev. Met.* 67(1970)77.
29. H. Schenck and K.W. Lange, *Arch. Eisenhüttenwes* 37(1966) 809.
30. L. Katz, M. Guinan and R.J. Borg, *Phys. Rev.* B4(1971) 330.
31. S. Scherrer, G. Lozes and B. Deviot, *C.R. Acad. Sci. B.* 264(1967)1499.
32. K.M. Olsen and C.F. Larkin, *J. Electron-Chem. Soc.* 110, 86(1963).
33. P. Cambette and P. Anzou, *C.R. Acad. Sci. Ser. C.* 267, 677(1969).
34. P. Cambette and Anzou, *Mem. Sci. Rev. Met.* 67, 17(1970).
35. W. Eichenauer, *Mem. Sci. Rev. Met.* 57, 943 (1960).
36. F.G. Jones and R.D. Pehlke, *Met. Trans.* 2(1971) 2655.
37. J.S. Blakemore, W.A. Oates and E.O. Hall, *Trans. TMS-AIME* 242(1968) 332.
38. H. Schenck and K.W. Lange, *Z. Metallkunde* 57(1966) 378.
39. M.L. Hill and E.W. Johnson: *Trans. Met. Soc. AIME* 215(1959) 717.
40. Schenck, H. and Taxhet, H., (1959), *Archiv. f. Eisenhüttenw* 30 p. 661.
41. Gorman, J.K. and Nardella, W.R., (1962), *Vacuum Vol.* 12. p. 19.
42. Bryan, W.L. and Dodge, B.F. *A.I. Ch. E.J.* 9(1963)223.
43. Wagner, R. and Sizman, R., *Z. Angew. Physik* 18(1964)193.
44. Heiarich, R.H. Johnson, C.E. and Crouthamel, C.F. *J.I-electro Chem. Soc.* 112(1965)1069.
45. Gonzalez, G.D. *Trans. Met. Soc. AIME*, 239(1967) 607.
46. Salli, V.L. Geld, P.V. and Ryabov. R.A., *Fiz. Khim. Mekh. Mater.* 6(1970)96.
47. Nelson, H.G. and Stein, J.E. *U.S.A. Report NASA-TN-D-7265.*
48. Kunnick, A.J. and Johnson, H.H. *Trans.* 6A(1975), 1087.
49. Miller, R.F., Hudson, J.B. and Ansell, G.S., *Met. Trans.* 6A(1975)117.
50. Louthan, M.R., Derrick, R.G., Donovan, J.A. and Caskey G.R., *Proc. Int. Conf. Effect of Hydrogen on Behaviour of Materials* (Eds. A.W. Thompson and I.M. Bernstein, *Met. soc. AIME*, 1976, p. 337.

51. Rumnick, A.J. and Johnson, H.H. *Acta. Met.* 25(1977) 891.
52. Quick, W.R and Johnson, H.H. *Acta. Met.* 26(1978) 903.
53. Gaggell, V.J. and Johnson, D.L. *J. Materials for Energy System* 1(1979)32.
54. Masui, K., Yoshida, H. and Watanabe, R. *Trans. Iron and Steel Inst. Japan.* 19(1979)547.
55. Waelbroeck, F, Ali-Khan, I., Dietz, K.J. and Weinhold, p., *Jl. Nucl. Mat.* 85/86(1979)345.
56. Riecke, E., *Werkst, U. Korros*, 32(1981)66.
57. T.M. Stross and F.C. Tompkins, *Diffusion Coefficient of Hydrogen in Iron.* *J. Chem. Soc.* p. 230(1956).
58. Jeiy, Choi, *Met. Trans. Vol. 1*, p. 911(1970).
59. Geller, W. and Sun, T.H. *Arch. Eisenhüttwes*, 21(1950)423.
60. Johnson, E.W. and Hill, M. *Acta. Metall.* 3(1955)99.
61. W. Beck, J.O'M. Bockris, J. McBreen and L. Nanis, 1965.
62. M.J. Puska and R.M Nieminen, *Phys. Rev. B(USA) Vol. 29, No. 10.* P. 5382-97 (1984).
63. D. Bergner, *Proceeding of International conference "Diffusion in Metals and Alloys" Tihany, Hungary 30 Aug - 3 Sept. 1982 (Aedermannsorf, Switzerland) P. 223-40.*
64. A. LeClair, *Diffusion in Metals II, Prog. in Metal Phys.* (Pergamon Press, London, 1953) Vol. 4.
65. C. Wert. *Phys. Rev.* 79, 601(1950).
66. R.M. Barrer, *Discussions. Faraday Soc.* 4, 48 (1948).
67. C. Wert and C. Zener, *Phys. Rev. Vol. 76, No. 8,* P. 1169(1949).
68. C. Zener, *Diffusion-Imperfections in Nearly Perfect Crystals* (John Wiley and Sons. Inc. New York, 1950).
69. A. Ferro, *J. Appl. Phys. Vol. 28, No.8,* P. 895 (1957)
70. Y. Adda and J. Philbert, *La. Diffusion dans les Solides Institut National des Sciences et. Techniques Nucleaires Saclay*, 1966 P. 1166 and 1168.
71. J.R.G. Da Silva and R.B. McLellan, *Met. Sci. Eng.* 26, 83(1976).

72. D.N. Beshers, In ASM Seminar on diffusion, Am. Soc. Met (1973) 209-240.
73. J. Vokl and G. Alefeld. Topics in Appl. Phys. Vol. 28 (1978) p. 321, Berlin.
74. C. Zener. In Imperfections in Nearly Perfect Crystals (Ed. W. Shockely, Wiley, 1952).
75. E.O¹.Wallan, J.W. Cable and W.C. Koehler, J. Phys. Chem. Solids 24, 1141 (1963).
76. J.F.Freedman and A.S. Nowick Acta. Met. Vol. 6(1958) p. 176-183.
77. H.B. Huntington, G.A. Shirn and E.S. Wajda: Phys. Rev. Vol. 99, No. 4(1955), P. 1085-1091.
78. W.A. Oates Met. Forum (Australia) Vol. 2, No. 3. P. 138-48 (1979).
79. W.A. Oates: Scr. Met. Vol. 6, P. 349-352 (1972).
80. C.I. Smithless, E.A. Brandes Metals reference Book, fifth Edition Butterworths London and Boston, 1976.
81. National Bureau of Standards Circular 500(1952) and K Burton and H.A. Krebs, Biochemical journal 54, 94(1953).
82. J.P. Hirth and J. Lothe, Theory of dislocation McGraw Hill Book Company (1968).
83. D.Hull, Introduction to dislocations Pergamon Press (1965).
84. R.A. Oriani: Acta. Met. 18(1970), 147-157.
85. J.B. Leblond and D. Dubois; Acta. Met. Vol. 31 No. 10, (1983), P. 1459-1469.
86. A. McNabb and P.K. Foster: Trans. Met. Soc. AIME 227(1963) 618.
87. Y. Sakamoto: Trans. of the Japan Institute of Metals 1984, Vol. 25, No. 4, p. 244-256.
88. M.R. Louthan, JR., J.A. Donovan and G.R. Caskey, JR., Scr. Met. June 1974.
89. R.M. Barrer, Trans. Faraday, Soc. 35(1939) 628.
90. J. Vokl and G. Alfeld: Diffusion in Solids, Eds. A.S. Nowick and J.J. Burton (Academic Press, New York, 1975) P. 231.
91. W. Koster, L. Bangort and R. Hahn, Arch. Eisenhutt enw 25, 569(1954).
92. A.S. Keh and S. Weissman, Electron Microscopy and Strength of Crystals, 231, Interscience New York (1963).
93. L.S. Darken and R.P. Smith Corrosion 5(1949).
94. A.J. Kunnick and H.H. Johnson: Acta. Met. 28(1980) 33.

95. G. Naeser and N. Dautzenberg, Arch. Eisenhüttenw 36, 175(1965).
96. J.G. Harhai, T.S. Viswanathan and H.M. Davis, ASM Trans. Quart. 58, 210(1965).
97. Y. Sakamoto and J. Eguchi: Proc. Japan Congress on Materials Research, 19(1976), p. 91.
98. G.M. Pressouyre and I.M. Bernstein: Acta. Met. 27(1979) 89.
99. G.M. Pressouyre and I.M. Bernstein: Met. Trans. 12A(1981), 835.
100. K. Kiuchi and R.B McLellan Acta. Met. 31(1983) 961.
101. G.M. Pressouyre: Acta. Met. 28 (1980) 895.
102. B. Chew, Metal. Sci. J. 5, 195(1971).
103. M. Koiwa, Acta. Met. 22, 91(1974).
104. K. Schroeder, Z. Physik, B25, 91(1976).
105. R.B. McLellan Act. Met. 27, 1655(1979).
106. R. Kirchheim, Acta. Met. 30, 1069 (1982).
107. C.N. Park, G.W Hong and J.Y. Lee Proc. of 3rd International Congress on Hydrogen and Material, No. E9 (1982) Paris, P. 509.
108. B.M. Mogutnov, I.A. Tomilin and L.A. Shvartzman, Thermodynamics of Fe-C alloys, Metallurgica Pub. Moscow (1972), In Russian.
109. A.D. LeClaire and A. Rabinovitch, Proc. International Conference on diffusion in Metals and alloys Tihany, Hungary, Aug. 30 - Sept. 3, 1982, Aedermannsdorf, Switzerland, Trans. Tech. Pub., 428(1983).
110. A.J. Martlock, Acta. Metall. 8, 132(1960).
111. R.A. Swalin: Thermodynamics of Solids, Second Edition John Wiley and Sons, Inc. (1962).
112. J. O'M. Bockris, W. Beck, M.A. Genshaw, P.K. Subramanyan and F.S. Williams, Acta. Metall. 19, 1209(1971).
113. J.P. Hirth and B. Carnhan, Acta. Metall. Vol. 26, P. 1795-1803, Pergamon Press, 1978, Printed in G.B.
114. Kidane Belai: M.Sc. Thesis.
115. A.D. LeClaire, Diffusion and defect data, Vol. 33, 1983, p. 1-66.
116. A.D. Le Claire, Diffusion and Defect Data, Vol. 34, 1983, p. 1-35.
117. Nicholas F. Fiore and Charles L. Bauer: Prog. in Mat. Sci. Vol. 13, No. 2(1968).
118. J. Burke: The Kinetics of Phase Transitions in Metals Pergamon Press London (1965).
119. W. Jost. Diffusion in Solids, Liquids and Gases Academic Press-New York (1960).